

Pb, Sr, and Nd isotopic characteristics of a variety of lithologies from the Guerrero composite terrane, west-central Mexico: constraints on their origin

Adriana Potra^{1,*}, Rosemary Hickey-Vargas², Andrew W. Macfarlane², and Vincent J.M. Salters³

¹ Department of Geosciences, University of Arkansas, Ozark Hall 22, Fayetteville, AR 72701, USA.

² Department of Earth and Environment, Florida International University, 11200 SW 8th Street, Miami, FL 33199, USA.

³ National High Magnetic Field Laboratory and Department of Earth, Ocean and Atmospheric Science, Florida State University, 1800 E Paul Dirac Dr, Tallahassee, FL 32310, USA.

* potra@uark.edu

ABSTRACT

Lead, Sr, and Nd isotope analyses of Mesozoic and Cenozoic rocks from the southern part of Guerrero terrane in Mexico provide a better understanding of their origin. Metamorphic rocks collected south of Arteaga (Zihuatanejo terrane) have similar Pb isotope values to basement rocks from Nevado de Toluca, indicating a possible connection of the basement in these areas. Lead isotope ratios of rocks from the Mesozoic Guerrero and Paleozoic Mixteca terranes are similar to those of north Peruvian Mesozoic Olmos and Paleozoic Marañoón complexes, but more radiogenic than Grenville-age basement of southeast Mexico (Guichicovi complex) and north Colombia (Garzón massif and Santa Marta massif).

Present-day Pb, Sr, and Nd isotope ratios of Mesozoic sedimentary rocks from Zihuatanejo and Teloloapan terranes define two clusters: rock from the Huetamo region (Zihuatanejo terrane), with less evolved isotopic signatures, and rocks from the Coastal belt (Colima and Purificación areas in Zihuatanejo terrane) and from the Teloloapan area (Teloloapan terrane) with higher isotopic ratios. Pb, Sr, and Nd isotopic ratios suggest the involvement of a more evolved component, possibly the basement rocks, in the generation of the sedimentary rocks from the Coastal belt and south of Teloloapan area compared to the sedimentary rocks from the Huetamo area.

Cenozoic plutonic rocks from La Verde have more radiogenic isotopic ratios than samples from Ingúarán, El Malacate, and La Esmeralda. These differences could result from assimilation of different rocks (Arteaga complex or sedimentary rocks) or different extents of contamination. Initial Sr and Nd isotopic values of the Cretaceous granitoids from Manzanillo and Jilotlán plot very close to the igneous samples from Ingúarán, El Malacate, and La Esmeralda; this similarity may indicate that they had a common source. Isotopic compositions of Cenozoic plutonic rocks are consistent with subduction-related magmatism and suggest involvement of crustal material by assimilation during the rise of the magma, or by incorporation of subducted sediments, or both.

Key words: radiogenic isotopes; thermal ionization mass spectrometer; multi-collector inductively coupled plasma mass spectrometer; Guerrero terrane; Zihuatanejo terrane; Mexico.

RESUMEN

Analisis isotópicos de Pb, Sr y Nd de rocas mesozoicas y cenozoicas de la parte sur del terreno Guerrero en México contribuyen una mejor comprensión de su origen. Rocas metamórficas colectadas al sur de Arteaga (terreno Zihuatanejo) tienen valores isotópicos de Pb similares a los de rocas del basamento del Nevado de Toluca, indicando una posible conexión del basamento en esas áreas. Las relaciones isotópicas de Pb de rocas de los terrenos Guerrero del Mesozoico y Mixteca del Paleozoico son similares a las de los complejos Olmos del Mesozoico y Marañoón del Paleozoico del Perú, pero más radiogénicas que las del basamento de edad grenvilliana del sureste de México (complejo Guichicovi) y del norte de Colombia (macizos Garzón y Santa Marta).

Las relaciones isotópicas actuales de Pb, Sr y Nd de rocas sedimentarias mesozoicas definen dos grupos: rocas de la región de Huetamo (terreno Zihuatanejo) con firmas isotópicas menos evolucionadas, y rocas del cinturón costero (áreas de Colima y Purificación en el terreno Zihuatanejo) y del área de Teloloapan (terreno Teloloapan) con relaciones isotópicas más elevadas. Las relaciones isotópicas de Pb, Sr y Nd sugieren la participación de un componente más evolucionado, posiblemente las rocas del basamento, en la generación de las rocas sedimentarias del cinturón costero y de la región al sur del área de Teloloapan, en comparación con las rocas sedimentarias del área de Huetamo.

Las rocas plutónicas cenozoicas de La Verde tienen relaciones isotópicas más radiogénicas que las muestras de Ingúarán, El Malacate y La Esmeralda. Esas diferencias pueden ser el resultado de la asimilación de diferentes rocas (complejo Arteaga o rocas sedimentarias) o de distintos grados de contaminación. Valores isotópicos iniciales de Sr y Nd de los granitoides cretácicos de Manzanillo y Jilotlán grafican muy cerca de las muestras ígneas de Ingúarán, El Malacate y La Esmeralda. Esta similaridad puede indicar que esas rocas tienen una fuente común. La composición isotópica de las rocas plutónicas cenozoicas es consistente con magmatismo relacionado a subducción y sugiere la participación de material cortical por procesos de asimilación durante el ascenso del magma o de incorporación de sedimentos subducidos, o ambos.

Palabras clave: isótopos radiogénicos; espectrómetro de masas de ionización térmica; espectrómetro de masas multicolector con plasma de acoplamiento inductivo; terreno Guerrero; terreno Zihuatanejo; México.

INTRODUCTION

More than 300 different tectonostratigraphic suspect terranes, whose presence reflects accretion-collision tectonics, have been recognized around the Circum-Pacific region (Howell *et al.*, 1983; Ben-Avraham, 1989). Their original paleogeography and origins are still intensely disputed; they may have formed elsewhere and subsequently accreted due to plate tectonics processes (Howell and Jones, 1989). The North American Cordillera forms the northeastern part of this circum-Pacific system of mountain chains, island arcs, trenches, and faults (Coney, 1989). It consists of (1) unmoved cratonic North American Precambrian basement and its late Precambrian to Jurassic miogeoclinal cover, and (2) rock assemblages found in the suspect terranes, whose lithotectonic assemblages record a very complex and variable history (Coney *et al.*, 1980).

The southern part of the Cordillera is located in Mexico and it records a very complicated evolution: in this region, features typical of Cordilleran tectonics are encountered, as well as elements of the Paleozoic Appalachian-Ouachita orogen and features related to the opening of the Gulf of Mexico in early Mesozoic time (Coney, 1989). Based on petrologic, tectonic, and geochronological differences in the Precambrian and Paleozoic basement, as well as on the petrologic and tectonic nature of Mesozoic terranes bordering the old continental nucleus, it has been suggested that southwestern Mexico consists of five tectonostratigraphic terranes: Guerrero, Mixteca, Oaxaca (the southernmost part of the larger Oaxaquia terrane), Juárez, and Xolapa (Figure 1) (Campa and Coney, 1983).

The Guerrero composite terrane (Figure 1) represents the second largest tectonostratigraphic unit of the Cordilleran collage of North America, after Wrangellia (Centeno-García *et al.*, 1993a). Debate continues over the paleogeographic evolution of this terrane and over the nature, origin, and evolution of its crustal rocks. Some authors (Lapierre *et al.*, 1992; Tardy *et al.*, 1994; Dickinson and Lawton, 2001)

favor the allochthonous models and argue that the Guerrero terrane is an exotic intra-oceanic arc proceeding from the paleo-Pacific domain whose accretion to the Mexican mainland during the late Early Cretaceous was triggered by the subduction and consumption of the oceanic Mezcalera plate (Dickinson and Lawton, 2001). The Mezcalera plate represented the basement of a large pre-Late Jurassic (Martini *et al.*, 2012) or pre-Late Cretaceous (Martini *et al.*, 2011) oceanic basin, named Arperos basin by Tardy *et al.* (1994). Talavera-Mendoza *et al.* (2007) postulate that the Guerrero terrane is a Jurassic-Cretaceous intra-oceanic multi-arc system developed in the paleo-Pacific domain along distinct subduction boundaries bordering the Mexican craton. In this scenario, the intra-oceanic arcs were separated from the continental margin by small oceanic basins that closed as the oceanic lithosphere was subducted, causing the accretion of the arcs to the mainland. Talavera-Mendoza *et al.* (2007) suggested that the accretion occurred during latest Cretaceous – early Paleogene, triggering the Laramide deformation across the Mexican Pacific margin. Yet other scientists (Lang *et al.*, 1996; Cabral-Cano *et al.*, 2000; Centeno-García *et al.*, 2008; 2011; Martini *et al.*, 2009, 2011) favor the para-autochthonous models, which suggest that the Guerrero terrane is a detached slice of the North American leading edge, which drifted out into the paleo-Pacific realm during the opening of the Late Jurassic – Early Cretaceous back-arc Arperos basin. The detachment was triggered by a great amount of extension (probably due to the rollback of the eastward subducting Farallon plate) that resulted in trenchward arc migration during the Late Cretaceous. Subsequently, the detached slice, more precisely the Zihuatanejo terrane (see Figure 1), was re-accreted to the nuclear Mexico between Santonian to Maastrichtian, during Laramide shortening (Centeno-García *et al.*, 2008).

In this study, we focus on the southern part of the Guerrero composite terrane, located south of the Trans-Mexican Volcanic Belt (TMVB), where the exposures of the Mesozoic arc assemblages are widespread. We present new Pb, Sr and Nd isotope results for

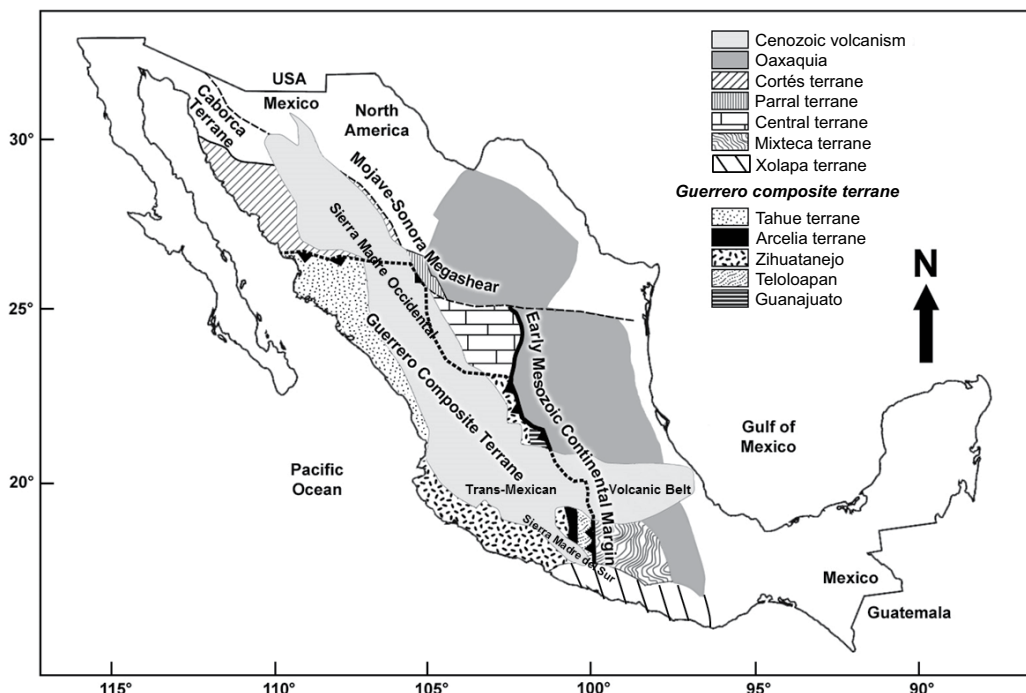


Figure 1. Schematic sketch of Mexico showing the Cenozoic volcanic cover (Sierra Madre Occidental, Sierra Madre del Sur, and the Trans-Mexican Volcanic Belt), the main tectono-stratigraphic terranes, and the distribution of the five terranes that belong to the Guerrero composite terrane (after Centeno-García *et al.*, 2008).

Mesozoic-Cenozoic metamorphic and sedimentary rocks, and for Cenozoic igneous rocks formed after accretion of the Guerrero terrane to nuclear Mexico. We also incorporate previously published data from south-east Mexico, North America and South America in order to provide a clearer picture of the provenance of the sampled rocks from the Guerrero terrane.

GEOLOGIC SETTING AND GEOCHEMICAL CHARACTERISTICS OF THE DOMINANT LITHOLOGICAL ASSEMBLAGES FROM THE TELOLOAPAN AND ZIHUATANEJO TERRANES

The Guerrero composite terrane (Figure 1) is mostly exposed in the Sierra Madre del Sur, south of the TMVB (which divides it into two major parts), and makes up most of western Mexico (Campa and Coney, 1983; Mendoza and Suástequi, 2000; Centeno-García *et al.*, 2008). North of the volcanic belt, most Guerrero terrane assemblages are covered by Cenozoic volcanic rocks of the Sierra Madre Occidental and are exposed only along the Pacific coast and in the Guanajuato and Zacatecas areas (Mendoza and Suástequi, 2000).

The Guerrero terrane consists of Late Jurassic (Tithonian)-Late Cretaceous (Cenomanian) volcanic-sedimentary arc sequences, and metamorphic complexes exposed in certain areas may represent their basement rocks (Centeno-García *et al.*, 1993a). The eastern portion of the Guerrero terrane was thrust over the Cretaceous platform carbonates or clastic sediments of the Mixteca terrane in Laramide time (Figure 1) (Campa-Uranga and Ramírez-Espinosa, 1979; Campa and Coney, 1983). The northeastern border is represented by continental margin strata of the Oaxaquia, Central, and Parral terranes (Figure 1) (Centeno-García *et al.*, 2008). Although the Guerrero terrane underlies most of western Mexico, the Mesozoic submarine volcano-sedimentary assemblages outcrop over less than five percent of its surface, being represented by erosional windows within the Cenozoic volcanic and sedimentary strata of the Sierra Madre Occidental, Sierra Madre del Sur, and TMVB (Mortensen *et al.*, 2008).

On the basis of differences in the dominant lithological assemblages, geochemical and isotopic characteristics, and inferred depositional ages, the Guerrero composite terrane has been subdivided into several subterranea (Campa and Coney, 1983; Sedlock *et al.*, 1993; Talavera-Mendoza *et al.*, 1995; Mendoza and Suástequi, 2000; Centeno-García, 2005; Centeno-García *et al.*, 2008). According to the latest subdivision (Centeno-García *et al.*, 2008), they are represented by the Zihuatanejo, Arcelia, and Teloloapan terranes, situated south of the Trans-Mexican Volcanic Belt, and the Tahue and Guanajuato terranes, located north of the volcanic axis (Figure 1). The northeastern part of the Zihuatanejo terrane, previously called the Zacatecas subterrane (Mendoza and Suástequi, 2000), is also located north of the volcanic belt (Figure 1). The Arcelia and Guanajuato terranes are distinctive by consisting of deep-marine sedimentary rocks and basaltic lava flows with primitive arc and OIB – MORB geochemical signatures (Centeno-García *et al.*, 2011). Scattered outcrops of basaltic pillow lavas and volcaniclastic turbidites exposed at Sierra de Guanajuato and Arcelia (Tardy *et al.*, 1994) have been interpreted as remnants of the Arperos basin and should mark the suture boundary between the Guerrero terrane and nuclear Mexico (Martini *et al.*, 2011). The two terranes that are relevant to the present study, the Teloloapan and the Zihuatanejo terranes, are described in more detail below.

The Teloloapan terrane

The eastern Teloloapan Terrane (Figure 1) is a 100 km wide and 300 km long N-S trending belt that is thrust over either Lower to mid-

dle Cretaceous carbonates or Upper Cretaceous clastic strata of the Mixteca terrane in a Laramide low-angle thrust fault (Campa-Uranga and Ramírez-Espinosa 1979; Campa and Coney, 1983). It consists of shallow-marine (east) and deeper (west) volcanic and sedimentary marine arc assemblages (Guerrero-Suástequi *et al.*, 1991; Talavera-Mendoza *et al.*, 1995; Mendoza and Suástequi, 2000).

On the eastern side, the lithostratigraphic column (Figure 2) consists of a more than 3000 m thick succession of Hauterivian-Aptian lavas (basalts, 85 %; andesites, 10 %; dacites-rhyolites, 5 %) and pillow breccias grouped into the Villa de Ayala Formation (Talavera-Mendoza *et al.*, 1995); this formation is capped by around 1500 m of Aptian to Turonian sedimentary cover (reefal limestone and volcaniclastic rocks; sandstone and shale) grouped into the Teloloapan and Pachivia formations (Campa-Uranga and Ramírez-Espinosa 1979; Mendoza and Suástequi, 2000; Guerrero-Suástequi, 2004; Centeno-García *et al.*, 2008). On the western side, characterized by deeper assemblages, the Villa de Ayala Formation is covered by Aptian-Cenomanian sedimentary sequences (volcanic shale and sandstone; deep-marine limestone; turbiditic sandstone-shale) of the Acapetlahuaya, Amatepec, and Miahuatepec formations (Figure 2) (Campa-Uranga and Ramírez-Espinosa, 1979; Talavera-Mendoza *et al.*, 1995; Guerrero-Suástequi, 2004; Centeno-García *et al.*, 2008).

The lavas (island arc calc-alkaline affinity) are enriched in LFSE (low-field strength elements) and LREE (light rare-earth elements), and show an important negative anomaly in Nb, Zr, and Ti typical of subduction-related suites (Mendoza and Suástequi, 2000). The $\epsilon_{\text{Nd}(t)}$ values of the Teloloapan terrane sequences (between +1.6 and +4.6) are more primitive compared to those of the adjacent Mixteca terrane and do not show influence of old continental crust in the magma generation (Centeno-García *et al.*, 1993a; Mendoza and Suástequi, 2000). Cabral-Cano *et al.* (2000) suggested that the arc volcanism of the Mixteca and Teloloapan terranes are part of a single arc-backarc system, with volcanism of the Mixteca terrane being related to the backarc basin. However, Guerrero-Suástequi (2004) interpreted these two terranes as being part of different arcs, separated by the double-dipping subduction of an oceanic basin.

According to Elías-Herrera and Sánchez-Zavala (1990/1992), the Tejupilco metamorphic suite, exposed in the Tejupilco and Taxco regions, may represent the basement of this terrane. Elías-Herrera *et al.* (2000) obtained ages for this suite that vary from Late Triassic (Carnian) to Late Jurassic (Oxfordian). The suite consists of more than 2000 m thick greenschist facies metamorphic rocks and a mylonitic augen gneiss of granitic composition called the Tizapa metagranite (Elías-Herrera *et al.*, 2000). Available Nd (initial ϵ_{Nd} of -3.5, and depleted mantle Nd model ages of 1.27 Ga) and Sr (initial $^{87}\text{Sr}/^{86}\text{Sr}$ of 0.7078) isotope data for the Tejupilco metamorphic suite suggest inherited Precambrian zircon in this unit (Elías-Herrera *et al.*, 2000).

The Zihuatanejo terrane

The western Zihuatanejo terrane (Figure 1), extending north of the TMVB and along the Pacific coast of Mexico, is the most extensively exposed Guerrero terrane, including a coastal belt, a basin at Huetamo, and a belt in central Mexico at Zacatecas (Ramírez-Espinosa *et al.*, 1991; Talavera-Mendoza *et al.*, 1993; Mendoza and Suástequi, 2000; Centeno-García *et al.*, 2008). Its basement consists of Triassic (Norian) quartz-rich turbidites (sandstone and shale) that form a matrix within which there are blocks of pillow basalts, diabase, banded gabbros, chert, and limestone (Campa *et al.*, 1982; Centeno-García *et al.*, 1993a, 1993b; Centeno-García *et al.*, 2008). These rocks have different names at different outcrops: Zacatecas Formation (near Zacatecas city), Arteaga Complex (around Arteaga city), Las Ollas Complex (near Zihuatanejo city), and Río Placeres Formation (near Huetamo)

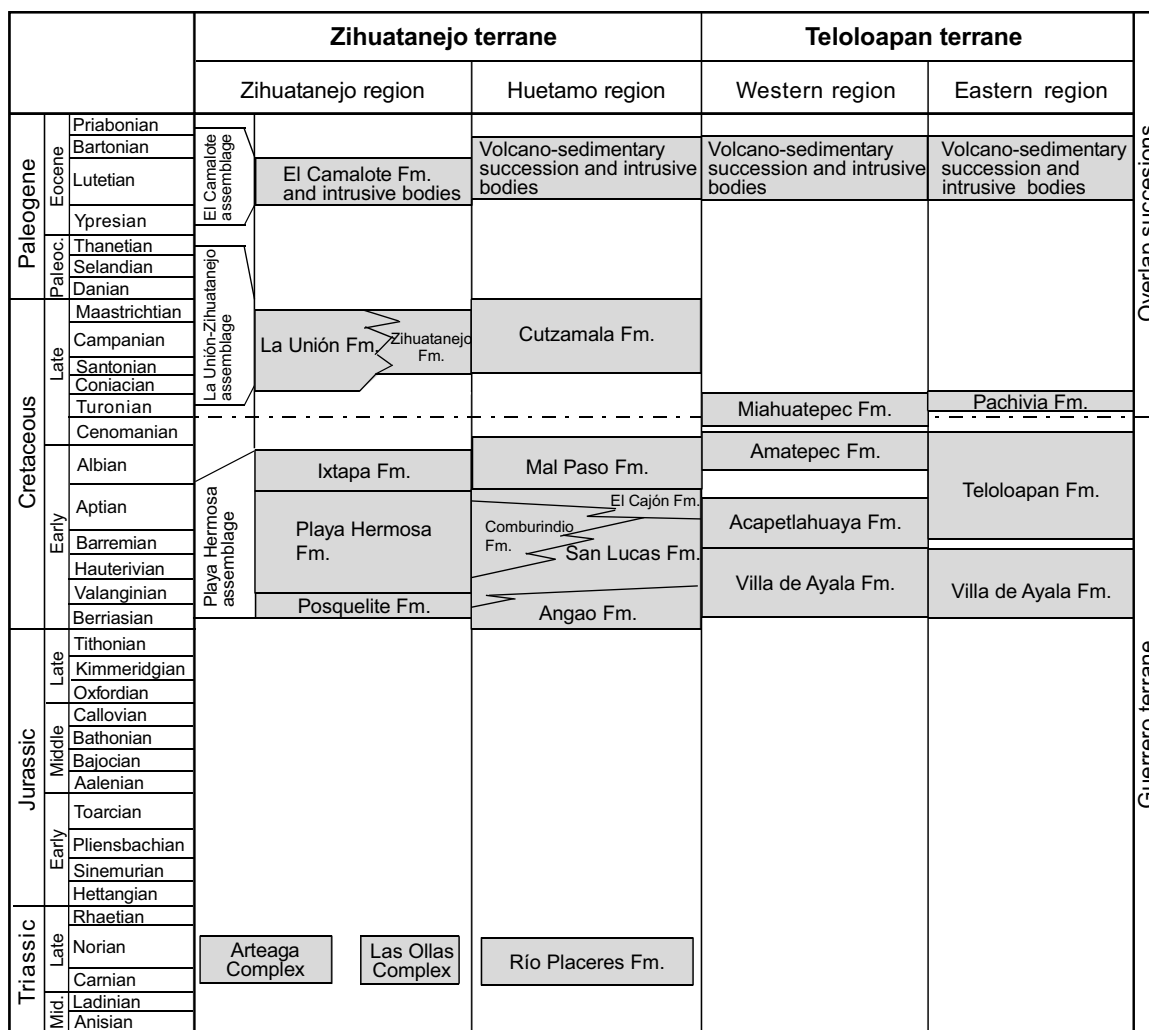


Figure 2. Chronostratigraphic columns of various regions from the Zihuatanejo and Teloloapan terranes (modified after Martini *et al.*, 2010). References for the Zihuatanejo region: Martini *et al.* (2010); for the Huetamo region: Guerrero-Suástequi (1997), Pantoja-Alor and Gómez-Caballero (2003), Martini *et al.* (2009); for the Teloloapan terrane: Campa and Ramírez (1979), Guerrero-Suástequi *et al.* (1991), Talavera-Mendoza *et al.* (1995), Guerrero-Suástequi (2004), Centeno-García *et al.* (2008).

(Burckhardt and Scalia, 1906; Centeno-García *et al.*, 1993a; Centeno-García and Silva-Romo, 1997; Talavera-Mendoza, 2000; Pantoja-Alor and Gómez-Caballero, 2003). Their metamorphism varies from none to high-greenschist and amphibolite facies; blueschist facies rocks have been found in the Las Ollas Complex (Talavera-Mendoza, 2000; Centeno-García *et al.*, 2003). These rocks are interpreted to represent an Upper Triassic(?) – Lower Jurassic subduction-related accretionary complex (Centeno-García *et al.*, 2008). The pillow lavas of the Arteaga Complex have $\epsilon_{\text{Nd(i)}}$ values higher than most MORBs (+13.1 and +13.2), and $^{87}\text{Sr}/^{86}\text{Sr}_{\text{(i)}}$ of 0.7047 and 0.7048 (Centeno-García *et al.*, 1993a); the sediments of the same complex ($\epsilon_{\text{Nd(i)}}$ of -6.2 and -7.2, and $^{87}\text{Sr}/^{86}\text{Sr}_{\text{(i)}}$ of 0.7163 and 0.7244), with a very distinctive sandstone composition that can help separating it from younger succession, suggest that they have been supplied from an evolved continental crust (Centeno-García *et al.*, 1993a).

The Middle-Late Jurassic and Early Cretaceous arc successions (Figure 2) range from Tithonian to Cenomanian in age and consist of andesitic, basaltic, and rhyolitic volcanic and volcanioclastic rocks, interbedded with limestone, evaporites, and red beds (Grajales and López, 1984). According to the latest subdivision (Martini *et al.*, 2010),

in the Zihuatanejo area this arc succession is grouped into the Playa Hermosa assemblage, while earlier studies (Vidal-Serratos, 1984; Mendoza and Suástequi, 2000) grouped it into the Zihuatanejo volcano-sedimentary sequence. The Playa Hermosa assemblage consists of the Early Cretaceous Posquelite, Playa Hermosa, and Ixtapa formations (Figure 2) (Martini *et al.*, 2010). In the Huetamo area, the arc assemblage consists of the Angao, San Lucas, Comburindio, El Cajón, and Mal Paso formations (Figure 2) (Pantoja-Alor, 1959; Guerrero-Suástequi, 1997; Pantoja-Alor and Gómez-Caballero, 2003), grouped into the Huetamo Sequence by Mendoza and Suástequi (2000).

The arc succession was deformed prior to the intrusion of large granitoids of latest Cretaceous to Paleogene age (Schaaf *et al.*, 1995). Late Cretaceous continental to shallow marine rocks (La Unión-Zihuatanejo assemblage in the Zihuatanejo area and Cutzamala Formation in the Huetamo area) (Figure 2) rest unconformably on all previous units (Centeno-García *et al.*, 2008; Martini *et al.*, 2010). It has been suggested (Martini *et al.*, 2010) that the Cretaceous layers are not part of the tectono-stratigraphic Guerrero terrane but rather represent an overlap succession that post-dates the possible accretion of this terrane to nuclear Mexico. The Upper Cretaceous units are

unconformably overlain by horizontally bedded Eocene volcanic and volcanioclastic rocks and intruded by large igneous bodies (Figure 2) (Martini *et al.*, 2010).

The geochemical signatures of the Lower Cretaceous andesite and dacite lava flows (island arc calc-alkaline affinity) of the Zihuatanejo Formation (Mendoza and Suástequi, 2000) are similar to those encountered in subduction-related tholeiitic and calc-alkaline magmatic suites: important negative anomalies in Zr and Ti, enrichment in LFSE and depletion in HFSE (high-field strength elements) relative to N-MORB, and enrichment in LREE relative to HREE (heavy rare-earth elements) (Mendoza and Suástequi, 2000). Available Sr and Nd isotopic data of two andesites ($\epsilon_{\text{Sr(i)}} = -2.6$ and -8.7 , and $\epsilon_{\text{Nd(i)}} = +8.1$ and $+8.3$) are typical of intra-oceanic arc suites (Freydier *et al.*, 1993). The scarce Berriasian-Valanginian basaltic lavas (island arc tholeiite affinity) of the Angao Formation in the Huetamo region (Guerrero-Suástequi, 1997) tend to show increasing LREE and LFSE enrichment relative to N-MORB from the bottom of the sequence to the top; all samples show negative anomalies in Zr and Ti, indicating provenance from an island-arc source (Mendoza and Suástequi, 2000). Overall, the geochemical and isotopic characteristics of the Cretaceous volcanic rocks suggest a transitional composition between oceanic island arcs and active continental margins, and are more evolved than rocks of the Teloloapan and Arcelia terranes (Freydier *et al.*, 1997; Mendoza and Suástequi, 2000; Centeno-García *et al.*, 2008). The presence of vertebrate fossils suggests proximity to the continent (Centeno-García *et al.*, 2008).

Post-accretional characteristics

The tectonic evolution of the Guerrero composite terrane during the Cenozoic is quite complex: from the early Paleogene and until around 29 Ma the Farallon plate was subducted eastward beneath southern Mexico; between 29 and 12.5 Ma subduction of the Guadalupe plate, formed by fragmentation of the Farallon plate, occurred; since approximately 12.5 Ma the Cocos and Rivera plates have been overridden by the North America plate along the Middle America (Acapulco) Trench (Schaaf *et al.*, 1995; Morán-Zenteno *et al.*, 1999).

The subduction of the Farallon plate beneath the North America plate created the NNW trending Sierra Madre Occidental (SMO) province (Figure 1), which records three different volcanic episodes (Morán-Zenteno *et al.*, 1999). The first one is the Laramide volcano-plutonic succession of the Lower Volcanic Supergroup (McDowell and Keizer, 1977) of Late Cretaceous to Paleogene age, made up of calc-alkaline, granodioritic to granitic batholiths that intrude volcanoclastic rocks (Morán-Zenteno *et al.*, 1999; Valencia-Moreno *et al.*, 2001). In the southern area, the batholith belt was emplaced into Mesozoic island-arc-related volcanic and sedimentary rocks of the Guerrero terrane (Valencia-Moreno *et al.*, 2001). The second and third volcanic episode in the SMO province formed the Upper Volcanic Supergroup (McDowell and Keizer, 1977) in early Oligocene and early Miocene time; rocks from this supergroup consist of silicic ignimbrites, rhyolitic domes, and basaltic to andesitic lavas (Morán-Zenteno *et al.*, 1999). The Cenozoic igneous rocks from La Verde, Ingurán, El Malacate, and La Esmeralda analyzed in this study are phases of the La Huacana granodiorite-quartz diorite pluton (Coochey and Eckman, 1978), which is part of the Cordilleran arc-related plutons and batholiths that extend from the Isthmus of Tehuantepec to Sinaloa-Sonora.

The southernmost outcrops of volcanic rocks belonging to the TMVB delineate the northern limit of the Cenozoic magmatic rocks of the Sierra Madre del Sur (Figure 1), formed during subduction episodes along the Pacific margin prior to, and partly contemporary with, the margin truncation due to the displacement of the Chortis block (for lo-

cation of this block, see Figure 6) (Schaaf *et al.*, 1995; Morán-Zenteno *et al.*, 2004). The displacement was responsible for the change from Sierra Madre del Sur magmatism to an E-W trending mafic to intermediate TMVB volcanism during the Miocene, around 16 m.y. ago (Schaaf *et al.*, 1995; Morán-Zenteno *et al.*, 2007). The intrusive rocks consist of a chain of calc-alkaline, dioritic to granitic batholiths commonly cut by silicic and mafic dikes, and smaller intrusive bodies that outcrop along the southwestern continental margin of Mexico (Morán-Zenteno *et al.*, 1999). The plutons from Sierra Madre del Sur intrude Mesozoic units ranging from volcano-sedimentary arc sequences of the Guerrero terrane to metagraywackes, quartz-amphibolites, quartz-feldspathic gneisses, and marble lenses in the Xolapa terrane (Figure 1) (Ortega-Gutiérrez, 1981; Schaaf *et al.*, 1995). The extrusive rocks are represented by a series of volcanic fields consisting of subalkaline rhyolites to basaltic andesites (Morán-Zenteno *et al.*, 1999; Martiny *et al.*, 2000).

SAMPLING AND METHODOLOGY

The samples for this study were collected in the summer of 1996 by A.W. Macfarlane, with the assistance of Cia. Minera Peñoles, S.A., from surface outcrops and mine workings. The location and brief descriptions of the samples are shown in Figure 3 and included in Appendix I, respectively. Rock samples (igneous, sedimentary, and metamorphic) lacking visible signs of weathering and alteration were selected for analysis, in order to minimize the effects of these late-stage processes.

Procedures for Pb isotope measurements

Whole-rock samples were chemically processed in the class 100 radiogenic isotope clean laboratory at Florida International University (FIU) in Miami. Approximately 500 mg of whole rock powder was dissolved in 3 ml of a 3:2 Optima grade (Fisher Scientific) HF-HBr mixture and allowed to sit overnight. Two ml of HBr were then added to the dissolved samples and evaporated in laminar flow boxes with 0.3 μm particle filter size (standard HEPA filter). The dried samples were re-dissolved in 0.5N HBr and dried down three times to ensure complete removal of HF. Four to 5 ml of 0.5N HBr was added to the samples, ultrasonicated for around 5 minutes, and transferred to clean, HNO_3 -leached, centrifuge tubes. The samples were centrifuged for about 15–20 minutes and the clear, liquid part of the samples (excluding the residue, if any, from the bottom part) was transferred to clean, HNO_3 -leached, centrifuge tube and diluted with 0.5N HBr to final volume of 10 ml and centrifuged twice (opposite sides) for about 15 minutes. The Pb was separated and purified using cation exchange columns and an HBr medium (Manhes *et al.*, 1978). Lead blank levels for water distilled at FIU, and for 0.5 N HBr and 0.5 N HNO_3 prepared from Seastar reagents are uniformly better than 1.2 pg/g.

Lead isotope ratios were determined by thermal ionization mass spectrometry on a VG-354 multicollector mass spectrometer, equipped with five Faraday cups. An amount of solution corresponding to 1 μg of Pb was loaded on outgassed rhenium (Re) single filaments with silica gel and phosphoric acid. The isotopic composition was determined by static multicollection and represents an average of 150 ratio measurement. The data were corrected for instrumental fractionation by comparison with replicate analyses of the National Bureau of Standards SRM-981 lead standard. Measured average values of 43 analyses of this standard are as follows: $^{206}\text{Pb}/^{204}\text{Pb}=16.9118$; $^{207}\text{Pb}/^{204}\text{Pb}=15.4475$ and $^{208}\text{Pb}/^{204}\text{Pb}=36.5756$. Normalization of these values against the average values published for that standard by Todt *et al.* (1996) ($^{206}\text{Pb}/^{204}\text{Pb}=16.9356$; $^{207}\text{Pb}/^{204}\text{Pb}=15.4891$; $^{208}\text{Pb}/^{204}\text{Pb}=36.7006$) yielded a correction for fractionation factor of 0.8 permil/amu. Replicate analy-

ses of standards and samples demonstrate the overall reproducibility to be better than ± 0.05 percent/amu; analytical errors are thus smaller than the symbols indicate.

Procedures for Sr and Nd isotope measurements

Whole-rock samples were processed in the Geochemistry Laboratory at the National High Magnetic Field Laboratory in Tallahassee, FL. Around 90 mg of sample powder was weighed in a clean beaker and 5-7 ml HF:HClO₄ (4:1) dissolution mix was added to it (the above quantity is needed to ensure complete digestion of the samples). The solution was covered and left overnight on the hot plate at 125 °C. The next day the beaker was opened and the temperature was slowly increased to around 220 °C to allow complete evaporation of the perchloric acid. Approximately 3 ml 6 N HCl was added while carefully washing down the beaker sides, and let evaporate to dryness at 120 °C. This 6 N HCl step was repeated twice to ensure removal of all perchloric acid. Then, 0.2 ml 2.5N HCl was added to the cooled dry sample. After one hour the solution was centrifuged at 15,000 rpm for around 2 minutes. The Sr and Nd separation chemistry followed the procedure described by Hart and Brooks (1977) and Richard *et al.* (1976), respectively.

Sr isotope ratios were determined by thermal ionization mass spectrometry on a Finnigan MAT 262 RPQ mass spectrometer, equipped with seven Faraday cups. Sr was loaded on outgassed tungsten (W) single filaments. The data were acquired by static multicollection and represented averages of between 77 and 167 isotope ratio measurements each (when the 2se on the average ratios reached

0.000007, the data acquisition was halted). Filament temperature ranged between 1400 °C and 1500 °C and the beam intensity of ⁸⁸Sr varied between around 3.5 and 8 V. The ⁸⁷Sr/⁸⁶Sr ratios were corrected for mass fractionation using ⁸⁶Sr/⁸⁸Sr = 0.1194. During the time period of our data acquisition, the ⁸⁷Sr/⁸⁶Sr for the Eimer and Amend (E&A) standard was measured at 0.708002 (n = 5) which agrees with the long term (years) average of the E&A standard (assumed “true” value of 0.70800). In most cases, the 2se of the ⁸⁷Sr/⁸⁶Sr ratio for samples and E&A standard was ± 0.000007 .

The Nd isotopic compositions were determined using a Thermo Finnigan NEPTUNE multi-collector inductively coupled plasma mass spectrometer. One milliliter high purity 2% HNO₃ was added to the dry Nd-separate and 300 μ l of the solution was placed in cleaned polypropylene vials just prior to the analysis. This solution was further diluted with 2% nitric acid to obtain a beam intensity of ¹⁴⁴Nd between 10 and 15 V. The sample was introduced into the plasma by an APEX introduction system (Elemental Scientific). The solution uptake rate by the nebulizer is 63 μ l/min. The reported ratios are the average of 60 measurements, four seconds long each. The 2se on the ¹⁴³Nd/¹⁴⁴Nd ratio was ± 0.000003 or ± 0.000004 . ¹⁴³Nd/¹⁴⁴Nd were normalized for instrumental mass fractionation using ¹⁴⁶Nd/¹⁴⁴Nd = 0.7219. ¹⁴³Nd/¹⁴⁴Nd value for the La Jolla standard over the course of data collection was 0.511838 (n = 27) which agrees with the long term average measured for this standard. Nd isotope ratios are normalized to 0.511850, resulting in a correction factor of +0.000012. Overall, the 2se on the standard varied between ± 0.000004 and ± 0.000008 and the beam intensity of ¹⁴⁴Nd ranged between 3.7 and 6.2 V.

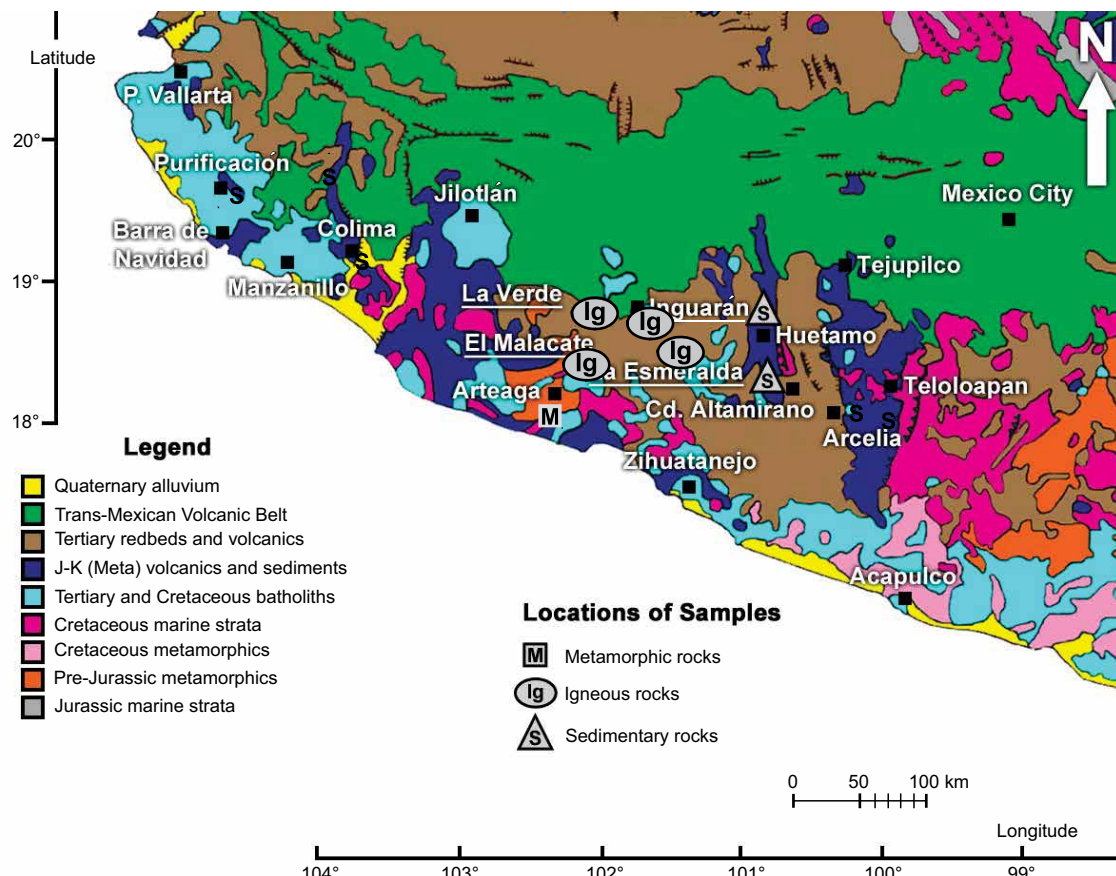


Figure 3. Locations where samples from the Guerrero terrane were collected, superimposed on the simplified geologic map of southwestern Mexico (geologic map modified after Lang *et al.*, 1996).

Procedures for trace element concentration analysis

Uranium, Th, Pb, Rb, Sr, Sm, and Nd concentrations were determined for a selected group of whole-rock samples. The whole-rock samples were chemically processed in the Department of Earth and Environment at FIU and their trace elements concentrations were determined at the Trace Evidence Analysis Facility at FIU, using a quadrupole ELAN DRC II inductively coupled plasma mass spectrometer operated in standard mode (Perkin Elmer LAS, Shelton, CT USA). Around 100 mg of sample powder was weighed in a 23 ml Savillex beaker, and 4 ml 8N HNO₃ and 2 ml HF were added to it. The solution was covered and heated to 150–200 °C for 8 hours after which it was dried down. Eight ml 8N HNO₃ was added to the dried sample and the beaker was capped and heated to 150–200 °C for 8 hours. Ten ml of double-distilled water was subsequently added. The mixture was heated up for at least 20 min, transferred to clean 250 ml polypropylene bottles, and diluted by 2000 times the original weight with double-distilled water. The diluted solution was shaken for about 45 min on a wrist-arm shaker. Ten ml of this solution was transferred to centrifuge tubes and part of it was used for trace elements measurements. Rock standards (BIR-1, DNC-1, W-2, BHVO-2, AGV-2, and QLO-1) were processed the same way and measured along with the samples in order to build calibration curves and constrain the accuracy and reproducibility of the measurements. The six standards were run three times in the sequence: at the beginning, midway, and at the end, with each measurement representing the average of three different readings. The first batch was used to build the calibration curves, and the average of the second and third ones (Appendix II) to constrain the accuracy and reproducibility of the data. For building the Pb and U calibration curves, all but the BHVO-2 standards were used. For building the Th calibration curve, only W-2, AGV-2, and QLO-1 standards were used. Replicate analyses of USGS standards for elements with available recommended values are all better than 2 % and have bias less than 7 % (Appendix II). Four blanks were run after the first batch of standards.

RESULTS

Radiogenic isotope compositions of Mesozoic-Cenozoic metamorphic and sedimentary rocks

Lead isotope ratios of five metamorphic rock samples collected south of Arteaga, part of the Zihuatanjo terrane (Figure 3), were measured. One of the samples, described as granoblastic schist (96MR107; Appendix I), may be part of one of the Cenozoic SW-NE shear zones that cut through the area; therefore, the age of the sample can be as young as Late Cretaceous to early Cenozoic (Centeno-García, personal communication). The results are given in Table 1 and shown in Figure 4. They have present-day Pb isotope values ranging between 18.854 and 18.995 for ²⁰⁶Pb/²⁰⁴Pb, 15.628 and 15.699 for ²⁰⁷Pb/²⁰⁴Pb, and between 38.894 and 39.204 for ²⁰⁸Pb/²⁰⁴Pb. In conventional Pb isotope plots, these values plot far to the right of the average Pb crust evolution curve of Stacey and Kramers (1975) and also to the right of the orogeny evolution curve of Zartman and Doe (1981) (Figure 4). On the ²⁰⁷Pb/²⁰⁴Pb vs. ²⁰⁶Pb/²⁰⁴Pb diagram, they generally plot below but close to the upper crust evolution curve of Zartman and Doe (1981) and are located to the right of the orogeny growth curve. Strontium and Nd isotope compositions were determined for two out of the previous five whole-rock metamorphic samples (Table 2), yielding ⁸⁷Sr/⁸⁶Sr values of 0.70838 and 0.72649, and ¹⁴³Nd/¹⁴⁴Nd ratios of 0.51257 and 0.51213 (Table 2). They plot in the enriched quadrant of the Sr-Nd correlation diagram (Figure 5).

Lead isotope ratios of thirteen sedimentary rocks from the Zihuatanjo terrane and three samples from the Teloloapan terrane

(Figure 3) were determined, the results being presented in Table 1 and shown in Figure 4. Present-day Pb isotope values of five siltstones, mudstone, and shale collected from the Coastal belt area of the Zihuatanjo terrane (Figure 3) range between 18.759 and 19.433 for ²⁰⁶Pb/²⁰⁴Pb, 15.585 and 15.648 for ²⁰⁷Pb/²⁰⁴Pb, and 38.498 and 38.880 for ²⁰⁸Pb/²⁰⁴Pb (Table 1 and Figure 4). Six sedimentary rocks (sandstones, siltstones, and shale) collected between Altamirano and Huetamo (Huetamo region; Figure 3) have present-day ²⁰⁶Pb/²⁰⁴Pb values between 18.626 and 18.994, ²⁰⁷Pb/²⁰⁴Pb between 15.568 and 15.646, and ²⁰⁸Pb/²⁰⁴Pb between 38.369 and 38.598 (Table 1 and Figure 4). Two other samples (siltstone and mudstone) collected near Huetamo show values of 18.626 and 18.763 for ²⁰⁶Pb/²⁰⁴Pb, 15.588 and 15.629 for ²⁰⁷Pb/²⁰⁴Pb, and 38.357 and 38.513 for ²⁰⁸Pb/²⁰⁴Pb.

Rocks from these two areas (Coastal belt and Huetamo region) of the Zihuatanjo terrane define two different clusters in conventional isotopic plots (Figure 4). On the thorogenic diagram, rocks from the Huetamo region plot between the orogeny and upper crust reservoir of Zartman and Doe (1981); samples from the Coastal belt area are shifted to more radiogenic values, plotting between the 0 Ma and 400 Ma values of the upper crust reservoir of Zartman and Doe (1981). On the uranogenic diagram, samples from the Huetamo region define a field located along the orogeny growth curve of Zartman and Doe (1981) and the Coastal belt rocks plot to the right of the same evolution curve (Figure 4). In both conventional isotopic plots, the Huetamo samples define a field below and close to the 0 Ma value of the average Pb crustal evolution curve of Stacey and Kramers (1975), whereas the Coastal belt samples plot far to the right of the same evolution curve (Figure 4).

Three meta-sedimentary samples from the Teloloapan terrane (sandstone and siltstone), collected south of Teloloapan (Figure 3), have present-day Pb isotope ratios ranging between 19.028 and 19.252 for ²⁰⁶Pb/²⁰⁴Pb, 15.649 and 15.652 for ²⁰⁷Pb/²⁰⁴Pb, and between 38.768 and 39.086 for ²⁰⁸Pb/²⁰⁴Pb (Figure 4). On conventional Pb isotope diagrams, they plot close to the rocks from the Coastal belt area of the Zihuatanjo terrane (Figure 4), suggesting similar Pb sources.

Sr and Nd isotope compositions were determined for five out of the previous sixteen whole-rock sedimentary samples. Two siltstones from the Coastal belt (96MR067 and 96MR069) have ⁸⁷Sr/⁸⁶Sr ratios of 0.70885 and 0.70936, and ¹⁴³Nd/¹⁴⁴Nd value of 0.51275 (Table 2 and Figure 5), plotting in quadrant I of the Sr-Nd isotopic correlation diagram. One siltstone sample collected between Altamirano and Huetamo (96MR117) has ⁸⁷Sr/⁸⁶Sr value of 0.70530 and ¹⁴³Nd/¹⁴⁴Nd of 0.51281 (Table 2), plotting above the $\epsilon_{\text{CHUR}}^{\text{Nd}}$ and to the right of the $\epsilon_{\text{UR}}^{\text{Sr}}$ (Figure 5). One mudstone sample (96MR127) from Huetamo yields isotopic ratios of 0.70758 for ⁸⁷Sr/⁸⁶Sr and 0.51257 for ¹⁴³Nd/¹⁴⁴Nd. In contrast to the siltstone sample, the Nd isotope ratio of the mudstone falls below that of Bulk Earth and plots in the enriched quadrant of the Sr-Nd isotope correlation diagram, implying that it might have been derived from more evolved crustal rocks (Figure 5).

Radiogenic isotope analyses of the Cenozoic igneous rocks

The Pb isotopic data for whole-rock igneous samples from La Verde (Figure 3 and Table 1) are from Potra and Macfarlane (2014). Additional samples from Ingurán, El Malacate, and La Esmeralda have been analyzed. They are shown in Table 1 and represented in Figure 4. Most of the samples are granodiorite, granite, diorite, and monzonite collected from porphyry copper deposits located in the central part of the Zihuatanjo terrane. A study by Barton *et al.* (1995) (and references therein) on porphyry copper and other intrusion-related mineralization in Mexico constrained the age of the intrusions from Ingurán and La Verde to around 35 Ma; therefore, when calculating the initial Sr and Nd isotopic ratios of the igneous samples, a 35 Ma was used (Table 3).

Table 1. Present-day Pb isotope compositions of analyzed samples and U, Th and Pb concentrations for a selected group of rocks from the Guerrero terrane.

Sample	Rock type	$^{206}\text{Pb}/^{204}\text{Pb}$ error (2 σ)	$^{207}\text{Pb}/^{204}\text{Pb}$ error (2 σ)	$^{208}\text{Pb}/^{204}\text{Pb}$ error (2 σ)	U (ppm)	Th (ppm)	Pb (ppm)				
Metamorphic rocks											
Zihuatanejo terrane	96MR101	schist	18.854	0.019	15.646	0.023	38.894	0.078	0.89±0.02	6.1±0.1	7.3±0.1
	96MR102	schist	18.977	0.019	15.628	0.023	38.924	0.078	N.D.	N.D.	N.D.
	96MR103	schist	18.953	0.019	15.670	0.024	39.063	0.078	N.D.	N.D.	N.D.
	96MR105	schist	18.995	0.019	15.679	0.024	39.190	0.078	1.78±0.04	11±0.2	5.7±0.1
	96MR107	schist	18.958	0.019	15.699	0.024	39.204	0.078	N.D.	N.D.	N.D.
Sedimentary rocks											
Zihuatanejo terrane – Coastal belt	96MR055	shale	19.047	0.019	15.648	0.023	38.535	0.077	N.D.	N.D.	N.D.
	96MR057	mudstone	19.433	0.019	15.640	0.023	38.880	0.078	N.D.	N.D.	N.D.
	96MR067	siltstone	18.997	0.019	15.606	0.023	38.783	0.078	1.34±0.03	3.72±0.07	2.66±0.05
	96MR068	siltstone	18.759	0.019	15.585	0.023	38.498	0.077	N.D.	N.D.	N.D.
	96MR069	siltstone	19.049	0.019	15.627	0.023	38.837	0.078	1.60±0.03	4.24±0.08	3.11±0.06
Zihuatanejo terrane – Huetamo region	96MR114	shale	18.994	0.019	15.633	0.023	38.598	0.077	N.D.	N.D.	N.D.
	96MR116	siltstone	18.645	0.019	15.646	0.023	38.575	0.077	N.D.	N.D.	N.D.
	96MR117	siltstone	18.626	0.019	15.568	0.023	38.369	0.077	1.21±0.02	3.12±0.06	4.77±0.09
	96MR118	siltstone	18.792	0.019	15.637	0.023	38.550	0.077	N.D.	N.D.	N.D.
	96MR119	sandstone	18.692	0.019	15.608	0.023	38.392	0.077	N.D.	N.D.	N.D.
Teloloapan terrane	96MR121	sandstone	18.701	0.019	15.587	0.023	38.470	0.077	N.D.	N.D.	N.D.
	96MR127	mudstone	18.763	0.019	15.629	0.023	38.513	0.077	1.32±0.03	2.75±0.05	5.7±0.1
	96MR128	siltstone	18.626	0.019	15.588	0.023	38.357	0.077	N.D.	N.D.	N.D.
	96MR129	(meta)siltstone	19.252	0.019	15.651	0.023	39.086	0.078	5.8±0.1	18.3±0.4	8.2±0.2
	96MR131	(meta)sandstone	19.029	0.019	15.652	0.023	38.795	0.078	N.D.	N.D.	N.D.
	96MR133	(meta)siltstone	19.028	0.019	15.649	0.023	38.768	0.078	N.D.	N.D.	N.D.
Cenozoic igneous rocks											
96MR071*	granodiorite	18.964	0.019	15.600	0.023	38.892	0.078	N.D.	N.D.	N.D.	
	diorite	18.986	0.019	15.570	0.023	38.699	0.077	N.D.	N.D.	N.D.	
	96MR078*	granodiorite	18.840	0.019	15.603	0.023	38.760	0.078	N.D.	N.D.	N.D.
	96MR079*	granodiorite	19.029	0.019	15.634	0.023	38.971	0.078	N.D.	N.D.	N.D.
	96MR083*	granodiorite	18.701	0.019	15.618	0.023	38.562	0.077	N.D.	N.D.	N.D.
	96MR088*	granite	18.879	0.019	15.659	0.023	38.862	0.078	6.3±0.1	25.7±0.5	20.6±0.4
	96MR095	granodiorite	18.835	0.019	15.626	0.023	38.742	0.077	4.23±0.08	17.5±0.3	8.5±0.2
	96MR096	granodiorite	18.761	0.019	15.625	0.023	38.651	0.077	3.36±0.07	12±0.2	11.7±0.2
	96MR096R**	granodiorite	18.761	0.019	15.625	0.023	38.651	0.077	3.11±0.06	11.3±0.2	12.5±0.2
	96MR099	granodiorite	18.772	0.019	15.544	0.023	38.461	0.077	6.2±0.1	22.2±0.4	11.6±0.2
	96MR099R***	granodiorite	18.766	0.019	15.533	0.023	38.440	0.077	6.2±0.1	22.2±0.4	11.6±0.2

N.D. = not determined; * Data from Potra and Macfarlane (2014); ** Replicate analysis (measured only for U, Th, and Pb concentrations); *** Replicate analysis (measured only for Pb isotope ratios).

Six granodiorite, granite, and diorite samples from La Verde have present-day $^{206}\text{Pb}/^{204}\text{Pb}$ values between 18.701 and 19.029, $^{207}\text{Pb}/^{204}\text{Pb}$ between 15.570 and 15.659, and $^{208}\text{Pb}/^{204}\text{Pb}$ between 38.562 and 38.971 (Table 1 and Figure 4). A granodiorite collected from Ingúarán (96MR095) shows isotopic ratios of 18.835 for $^{206}\text{Pb}/^{204}\text{Pb}$, 15.626 for $^{207}\text{Pb}/^{204}\text{Pb}$, and 38.742 for $^{208}\text{Pb}/^{204}\text{Pb}$. Two granodiorite samples from the small porphyry copper mine called El Malacate (96MR96) and from La Esmeralda (96MR99) display values of 18.761 and 18.772 for $^{206}\text{Pb}/^{204}\text{Pb}$, 15.625 and 15.544 for $^{207}\text{Pb}/^{204}\text{Pb}$, and 38.651 and 38.461 for $^{208}\text{Pb}/^{204}\text{Pb}$. The Pb isotope range of the igneous rocks resembles that of the orogenic reservoir in the plumbotectonics model of Zartman and Doe (1981), although a few samples from La Verde are shifted to more radiogenic values (Figure 4). On both conventional isotopic diagrams, the samples plot to the right of the average Pb crust evolution curve of Stacey and Kramers (1975).

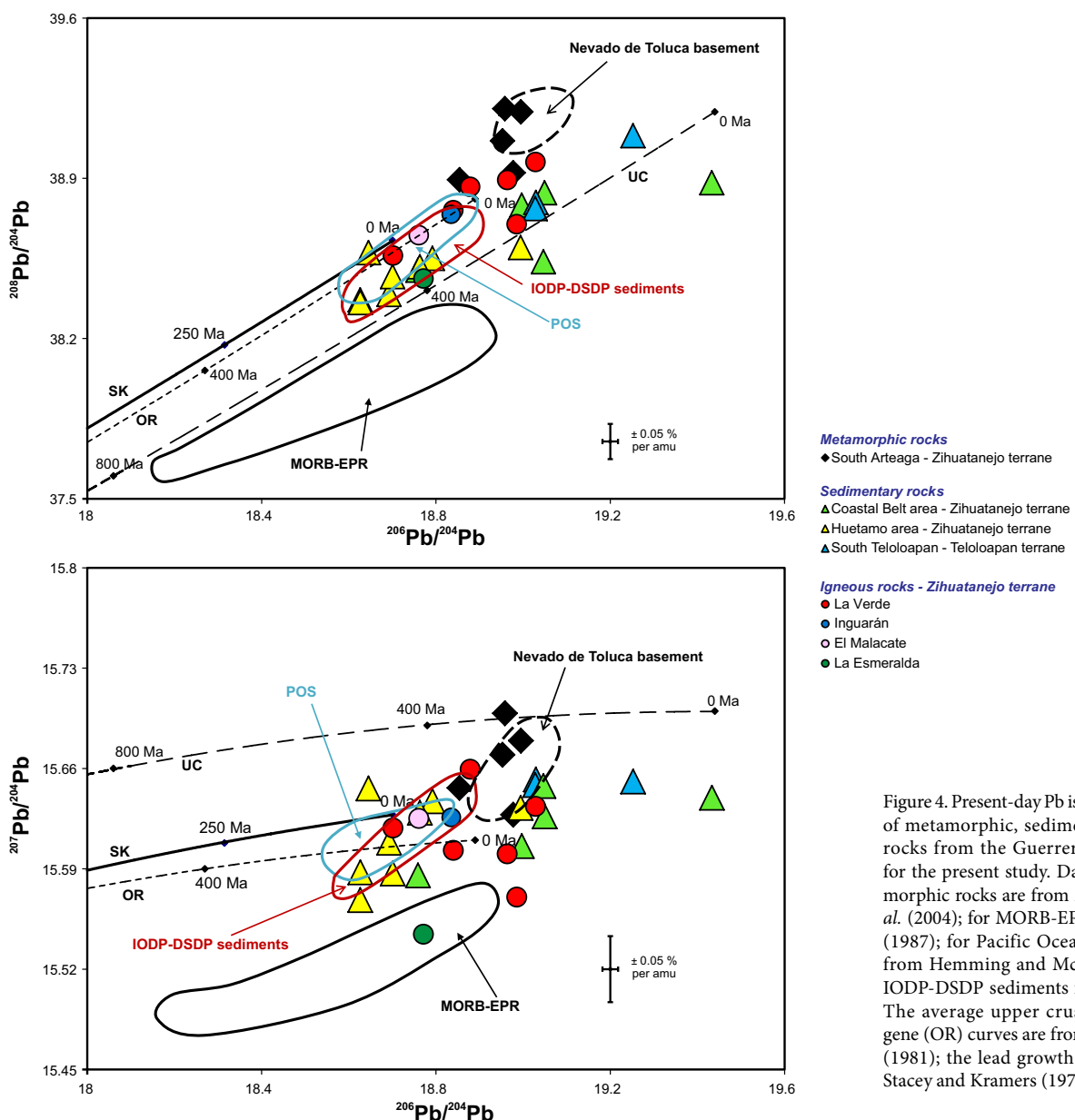
Sr and Nd isotope compositions were determined for four out of the previous nine whole-rock igneous samples (Table 2 and Figure 5). One Cenozoic granite sample collected from the La

Verde (96MR088) quarry yields $^{87}\text{Sr}/^{86}\text{Sr}$ of 0.70878 and $^{143}\text{Nd}/^{144}\text{Nd}$ of 0.51264. One massive granodiorite from Ingúarán has isotopic ratios of 0.70491 for $^{87}\text{Sr}/^{86}\text{Sr}$ and 0.51277 for $^{143}\text{Nd}/^{144}\text{Nd}$. Two Cenozoic granodiorite samples from the El Malacate mine and from La Esmeralda display values of 0.70491 and 0.70576 for $^{87}\text{Sr}/^{86}\text{Sr}$, and both have 0.51277 for $^{143}\text{Nd}/^{144}\text{Nd}$. The narrow ranges and generally low $^{87}\text{Sr}/^{86}\text{Sr}$ ratios, and $^{143}\text{Nd}/^{144}\text{Nd}$ values above that of Bulk Earth, of the igneous rocks from Ingúarán, El Malacate, and La Esmeralda suggest a relatively low degree of crustal contamination. In contrast, the isotopic values for the La Verde site may indicate more crustal contamination or a more evolved crustal component (Figure 5).

DISCUSSION

Isotopic characteristics of metamorphic and sedimentary rocks

Present-day Pb isotope ratios of metamorphic rocks collected south of Arteaga (Figure 6 - location 5) resemble those of metamorphic



xenoliths (represented by phyllite, schist, and gneiss) from continental crust beneath Nevado de Toluca volcano (Martínez-Serrano *et al.*, 2004; Figure 6 - location 4, and Figure 7); this may indicate a possible connection of the basement in these areas. They are also similar to the Pb isotopic compositions of rocks (mainly schist) of the Paleozoic Acatlán Complex (Martiny *et al.*, 1997), which is the basement of the Mixteca terrane (Figure 6 - location 6, and Figure 7). Metamorphic basement rocks from the northern Peruvian Olmos and Marañón Complexes (155 Ma and 435 Ma, respectively) (Figure 6 - locations 12 and 13), represented mainly by schist, have Pb isotope compositions (Macfarlane and Petersen, 1990) similar to metamorphic basement from the Mixteca (Martiny *et al.*, 1997) (Figure 7). Considering that these blocks have similar isotopic ages, it is possible that they had been related spatially and shared a common history prior to ending up in their current location.

Overall, present-day Pb isotope compositions of the analyzed metamorphic rocks are substantially more radiogenic than published

data (Martiny *et al.*, 2000) on high-grade metamorphic rocks (metagabbro and charnockite) from the Grenvillian-age Oaxaca terrane (Figure 7). On conventional Pb isotope diagrams, the samples from the Oaxaca Complex plot in a narrow range below the average Pb crust evolution curve of Stacey and Kramers (1975), close to the 1000 Ma field of the growth curve, whereas samples from both metamorphic suites in the Guerrero terrane plot to the right of the curve, falling in a more scattered area (Figure 7). The nonradiogenic Pb isotope compositions of the granulites from the Mesoproterozoic Oaxaca Complex (Figure 6 - location 7), the oldest known metamorphic belt in southern Mexico (900 – 1100 Ma; Ortega-Gutiérrez *et al.*, 1977), is related to the loss of U during the Grenville orogeny.

Present-day Pb isotope compositions of whole rocks from the Grenville-age Oaxaca Complex are within the field of Grenville-age rocks in the Santa Marta Massif in northernmost Colombia (Figure 6 - location 9, and Figure 7). Samples from the Mesoproterozoic Guichicovi Complex, exposed at the boundary between the Maya

Table 2. Present-day Sr and Nd isotope compositions and Rb, Sr, Sm, and Nd concentrations for a selected group of rocks from the Guerrero terrane.

Sample	Rock type	$^{87}\text{Sr}/^{86}\text{Sr}$	2se	$^{143}\text{Nd}/^{144}\text{Nd}$	2se	Rb (ppm)	Sr (ppm)	Sm (ppm)	Nd (ppm)	$^{87}\text{Rb}/^{86}\text{Sr}$	$^{147}\text{Sm}/^{144}\text{Nd}$
Metamorphic rocks											
<i>Zihuatanajo terrane</i>											
96MR101	schist	0.70838	7.00E-06	0.51257	2.76E-06	51±1	83±2	4.08±0.08	18.5±0.4	1.791	0.132
96MR105	schist	0.72649	7.00E-06	0.51213	2.72E-06	104±2	59±1	6.5±0.1	33.7±0.7	5.142	0.116
Sedimentary rocks											
<i>Zihuatanajo terrane - Coastal belt</i>											
96MR067	siltstone	0.70885	7.00E-06	0.51275	3.83E-06	68±1	98±2	3.75±0.07	16.7±0.3	2.008	0.135
96MR069	siltstone	0.70936	7.00E-06	0.51275	2.88E-06	77±2	89±2	3.78±0.07	16.1±0.3	2.518	0.141
<i>Zihuatanajo terrane - Huetamo region</i>											
96MR117	siltstone	0.70530	7.00E-06	0.51281	3.31E-06	11.1±0.2	349±7	2.89±0.06	14.1±0.3	0.092	0.123
96MR127	mudstone	0.70758	1.00E-05	0.51257	3.14E-06	64±1	189±4	2.57±0.05	11.9±0.2	0.975	0.130
<i>Teloloapan terrane</i>											
96MR129	(meta)siltstone	0.72295	7.00E-06	0.51268	2.87E-06	209±4	53±1	5.2±0.1	23.4±0.5	11.315	0.133
Cenozoic igneous rocks											
96MR088	granite	0.70878	7.00E-06	0.51264	2.68E-06	321±6	146±3	5.6±0.1	27.3±0.5	6.363	0.124
96MR095	granodiorite	0.70486	7.00E-06	0.51277	3.58E-06	104±2	195±4	5.1±0.1	23.6±0.5	1.539	0.129
96MR096	granodiorite	0.70491	7.00E-06	0.51277	3.75E-06	149±3	249±5	4.52±0.09	20.8±0.4	1.705	0.130
96MR096R*	granodiorite	0.70491	7.00E-06	0.51277	3.75E-06	145±3	250±5	4.54±0.09	21.1±0.4	1.705	0.130
96MR099	granodiorite	0.70576	7.00E-06	0.51277	2.51E-06	206±4	162±3	8.2±0.2	37.4±0.7	3.673	0.132

* Replicate analysis (measured for Rb, Sr, Sm, and Nd concentrations).

and the Juárez terranes (Figure 6 - location 8), have highly heterogeneous Pb isotopic values (Ruiz *et al.*, 1999) and define a field lying along the average Pb crustal growth curve and close to the field, also quite heterogeneous, defined by samples from the Garzón Massif, the southernmost Colombian Grenville-age massif (Figure 6 - location 11, and Figure 7). This led Ruiz *et al.* (1999) to consider that these now widely-separated basement blocks shared a common history in the late Proterozoic: the Oaxaca Complex with the Santa Marta Massif, and the Guichicovi Complex with the Garzón Massif. It has been suggested (Yañez *et al.*, 1991; Restrepo-Pace *et al.*, 1997; Ruiz *et al.*, 1999) that they were part of Gondwana during the early Paleozoic, and that the Oaxaca and Guichicovi complexes were transferred from that part of northwestern Gondwana presently occupied by Colombia to the southern end of Laurentia during Paleozoic orogenies related to the opening and closing of the proto-Atlantic Ocean.

Overall, it appears that common occurrences of higher $^{206}\text{Pb}/^{204}\text{Pb}$ and $^{207}\text{Pb}/^{204}\text{Pb}$ are present on the western side of Mexico (Nevado de Toluca xenoliths, and exposures in the Acatlán Complex from the Mixteca terrane, and metamorphic rocks south of Arteaga) and northern Peru (with exposures of the Olmos and Marañón complexes), whereas areas of lower $^{206}\text{Pb}/^{204}\text{Pb}$ and $^{207}\text{Pb}/^{204}\text{Pb}$ are located on the southeastern part of Mexico (with exposures of the Oaxaca and Guichicovi complexes) and Colombia (Santa Marta and Garzón massifs). The radiogenic Pb in rocks from the Mixteca terrane, Guerrero terrane, and the north Peruvian complexes, reflecting a history of elevated U/Pb relative to bulk earth models, reveal a different history from that of the ancient Oaxaca terrane, Guichicovi Complex, and the Colombian massifs, which reflect variable depletion of U relative to Pb.

Two schist samples collected south of Arteaga plot within the enriched quadrant of the Sr-Nd isotopic correlation diagram and show variable ratios (Figure 5), implying a larger interaction of the source rocks with the crust. One of the samples plots close to the field defined by rocks (sandstone and shale) of the Arteaga Complex (Centeno-García *et al.*, 1993a), suggesting a common source (Figure 5). The field defined by these two schist samples also resembles the field defined by xenoliths found in the Lower Toluca pumice of Nevado de

Toluca volcano (Martínez-Serrano *et al.*, 2004) (Figure 5). The similar Pb, Sr, and Nd isotopic ratios of metamorphic rocks collected south of Arteaga and Nevado de Toluca xenoliths suggest that they had been derived from a similar evolved continental source. Neodymium isotope results of Pepechuca high-grade gneiss xenoliths found in a Cenozoic volcanic field (La Goleta), around 50 km SW of Nevado de Toluca, indicate continental affinity ($\epsilon_{\text{Nd}} = -6.7$ and -7.3 and T_{DM} of 1.54 and 1.79 Ga; Elías-Herrera *et al.*, 1996) and are similar to values of Grenvillian rocks in Mexico. The basement rocks (phyllite, schist, and gneiss) under Nevado de Toluca have similar T_{DM} between 1 and 1.8 Ga (Martínez-Serrano *et al.*, 2004). These results and the similar Pb isotope ratios of the Toluca metamorphic rocks to those of the rocks collected south of Arteaga (Figure 4) suggest that the old component in the latter rocks may have been derived from the Grenville belt that extends from central Chihuahua to Oaxaca. Grenville-age rocks outcrop widely along the entire Appalachian Province (King, 1959) and continue south into Mexico (Ortega-Gutiérrez, 1981), but the cratonic rocks of Sonora, northern Chihuahua, and western United States are not suitable as primary sources for the sediments because they have much older T_{DM} (1.7–2.3 Ga) (DePaolo, 1981; Ruiz *et al.*, 1988a; Nelson and Bentz, 1990; Centeno-García and Silva-Romo, 1997). These results indicate the existence of an old (pre-Mesozoic) continental crust under the south-western part of Mexico, which was covered by Mesozoic arc sequences of the Guerrero terrane. It has been suggested (Centeno-García *et al.*, 2011) that the basement of the Zihuatanajo terrane has abundant Grenville, Pan-African, and Permian zircon populations, considered to have a Gondwanan / eastern Mexican signature, and therefore the Guerrero terrane is not exotic to mainland Mexico.

Isotopic dating of garnets (Sm-Nd) and hornblende (K-Ar) from four Grenvillian exposures in eastern and southern Mexico (Los Filtros metagranites and amphibolites, Novillo Gneiss, Huiznopala Gneiss, and Oaxaca Complex; Figure 6 - locations 1, 2, 3, and 7) yield metamorphic cooling ages between 0.9 and 1 Ga (Patchett and Ruiz, 1987; Ruiz *et al.*, 1988a; Ruiz *et al.*, 1988b). These imply a cooling history following Grenville metamorphism (1.05 – 1 Ga). T_{DM} for the same exposures vary between 1.37 and 1.6 Ga, which led Patchett and Ruiz

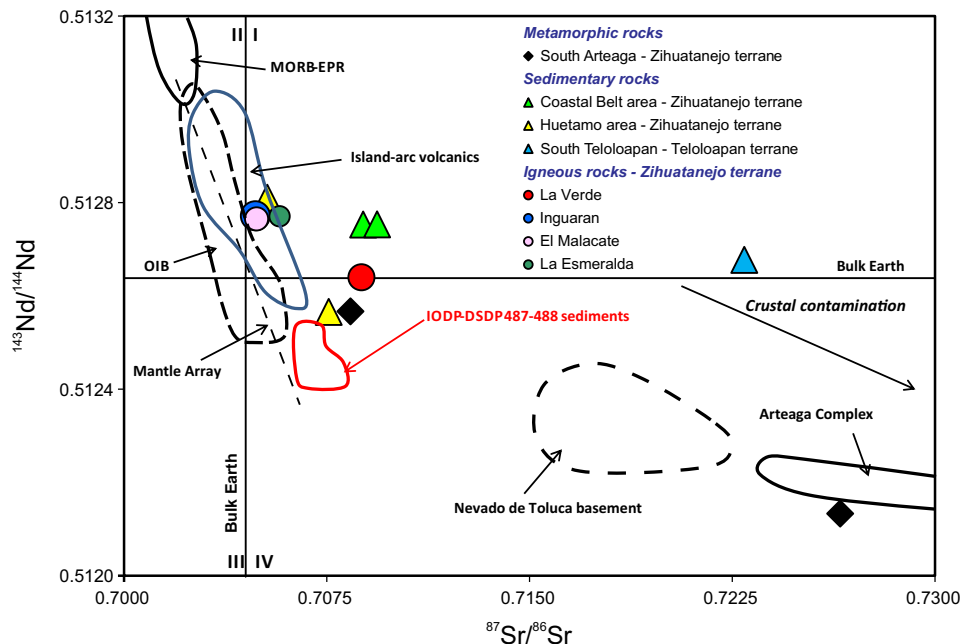


Figure 5. Strontium and Nd isotopic compositions of metamorphic, sedimentary, and igneous rocks from the Guerrero terrane analyzed for the present study. Data for building the IODP-DSDP 487-488 sediments field are from Verma (2000), for the Nevado de Toluca basement field from Martínez-Serrano *et al.* (2004), and for the Arteaga Complex field from Centeno-García *et al.* (1993a).

(1987) to conclude that these basement rocks originated from crustal protoliths that had been separated from the mantle roughly 0.5 Ga before the Grenville orogeny. The same authors suggested that the Mexican Precambrian outcrops represent mixtures between recycled Proterozoic crustal material and around 80 % of new material derived from the mantle during 1.1–1 Ga, as a result of tectonic and magmatic processes during the Grenville orogeny.

According to Centeno-García *et al.* (2011) and references therein, the stratigraphic section in the north-central part of the Huetamo area, part of an inland belt of the Zihuatanejo terrane, where two of our samples were collected (Appendix I, samples near Huetamo), is up to 4600 m thick and ranges in age from Kimmeridgian to Cenomanian. The upper part of the sequence is represented by 1000 m of shallow-marine clastic and calcareous rocks of the Mal Paso Formation, of Albian – Cenomanian age (Pantoja-Alor, 1959; Martini *et al.*, 2009). The section in the southern Huetamo, the region where six of our samples were collected (Appendix I, samples collected between Altamirano and Huetamo), is only about 800 m thick and contains the Mal Paso Formation that ranges in age from early Albian (clastic lower member) to early Cenomanian (calcareous member); this formation unconformably overlies the basement rocks represented by the Triassic Arteaga Complex (Centeno-García *et al.*, 2011). In the Colima area, part of the Coastal belt of the Zihuatanejo terrane, where three of our sedimentary rocks were collected (Appendix I, samples collected south of Colima), non-marine rocks of the Cerro de la Vieja Formation (Santonian – Maastrichtian) form a more than 500 m thick section of sandstone, conglomerate, and siltstone, with silicic lava flows in the middle part of the section (Centeno-García *et al.*, 2011). This formation may be part of a compressional arc assemblage that developed atop three older assemblages: (1) a Triassic – early Jurassic accretionary complex (Arteaga complex), (2) a Jurassic – earliest Cretaceous extensional arc assemblage, and (3) an early Cretaceous extensional arc assemblage (Centeno-García *et al.*, 2011).

The sedimentary rocks from the Zihuatanejo terrane sampled in

the study area define two different clusters on conventional present-day Pb isotope diagrams, with samples from the Huetamo area being less radiogenic than samples from the Coastal belt area (Figure 4). Samples from the Huetamo area plot close to the radiogenic end of the MORB-East Pacific Rise (EPR) field (White *et al.*, 1987) and are very similar to the published data for the sediments from the IODP-DSDP Leg 66 Sites 487 and 488, Cocos Plate (Verma, 2000) and for the Pacific Ocean sediments (Hemming and McLennan, 2001) (Figure 4). The samples from this sequence plot close to the 0 Ma field of the Stacey and Kramers (1975) Pb growth curve and define a narrow field just below this reference line; overall, they are fairly typical of the orogen reservoir of Zartman and Doe (1981).

In the Teloloapan area, the approximately 3000 m thick succession of volcanic succession (Hauterivian-Aptian) is capped by around 1500 m of Albian – early Cenomanian sedimentary cover represented by greywacke and tuffaceous shale, reefal and bioclastic limestones, and flysch-like sandstone and shale (Campa-Uranga and Ramírez-Espinosa 1979; Guerrero *et al.*, 1990; Mendoza and Suárez, 2000). Samples from this area have similar Pb isotope ratios, and on the Sr-Nd isotopic correlation diagram they plot within the same quadrant, as samples collected along the Coastal belt area of the Zihuatanejo terrane (Figure 5), suggesting similar sources. Pb, Sr, and Nd isotopic ratios suggest

Table 3. Time-integrated* Sr and Nd isotope ratios for the analyzed cenozoic igneous rocks from the Guerrero terrane.

Sample	$^{87}\text{Sr}/^{86}\text{Sr}$	$^{143}\text{Nd}/^{144}\text{Nd}$
96MR088	0.705621	0.512612
96MR095	0.704095	0.512743
96MR096	0.704062	0.512735
96MR099	0.703929	0.512741

* Initial Sr and Nd ratios were recalculated with ages of 35 Ma for the igneous rocks (see text for discussion).

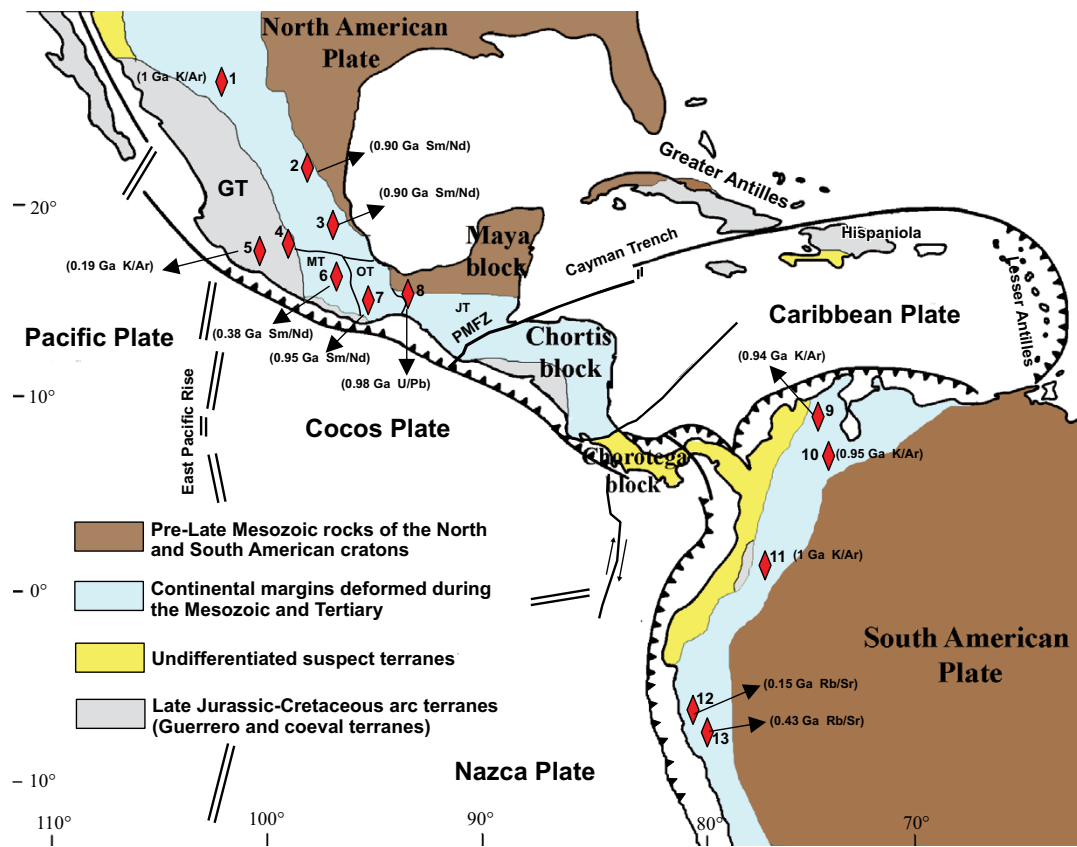


Figure 6. Structural schematic map of the North and South American Cordilleras showing the locations of basement exposures (and in parentheses their isotopic ages) discussed in this study (1 through 13). GT = Guerrero terrane; MT = Mixteca terrane; OT = Oaxaca terrane; JT = Juárez terrane; 1 = Los Filtros; 2 = Novillo Gneiss; 3 = Huiznopal Gneiss; 4 = Nevado de Toluca; 5 = Arteaga Complex; 6 = Acatlán Complex; 7 = Oaxaca Complex; 8 = Guichicovi Complex; 9 = Santa Marta Massif; 10 = Santander Massif; 11 = Garzón Massif; 12 = Olmos Complex; 13 = Marañón Complex (modified after Tardy *et al.*, 1994 and Sundblad *et al.*, 1991). References for isotopic ages and the minerals/rocks used (where information is available): 1: Mauger *et al.*, 1983 (hornblende); 2, 3, and 7: Patchett and Ruiz, 1987 (garnet); 5: Grajales and López, 1984 (metapelites); 6: Yáñez *et al.*, 1991 (garnet); 8: Ruiz *et al.*, 1999 (zircon); 9 and 10: Restrepo-Pace *et al.*, 1997; 11: Alvarez and Cordani, 1980; 12 and 13: Macfarlane, 1999 (whole-rock).

the involvement of a more evolved component in the generation of the sedimentary rocks from the Coastal belt and south of Teloloapan areas compared to the ones from the Huetamo area. One possibility would be involvement of the more radiogenic basement rocks of the Arteaga Complex, maybe to a lower extent for the south Huetamo rocks and to a larger extent for the south Colima and Purificación (Coastal belt area) rocks.

Isotopic characteristics of Cenozoic igneous rocks

Lead in plutonic rocks from the La Verde area is more radiogenic than any other analyzed igneous rocks from the Guerrero terrane, plotting along and to the right of the orogene reservoir of Zartman and Doe (Figure 4). The isotopic compositions of Pb in the igneous rocks from La Verde are compatible with derivation from ocean-floor basalts from the Cocos plate that have been enriched with radiogenic Pb (Figure 4). Since the Pb isotopic composition is close to the field defined by metamorphic xenoliths representing the basement under Nevado de Toluca (Figure 4), and this may be correlated with the basement under La Verde area, the radiogenic component may have been contributed by the basement rocks. Sr and Nd isotopic results (Figure 5) correlate well with the Pb isotopic results. On the Sr-Nd isotopic correlation diagram, the igneous sample from La Verde suggests a certain degree of evolved crustal contamination, which appears to be the basement represented by the Arteaga complex (Figure 5).

Subduction-related igneous rocks from Ingurán, La Esmeralda, and El Malacate have Pb isotope compositions that overlap the isotopic compositions of both, subduction sediments and sedimentary rocks from the Huetamo area (Figure 4). Lead in subducted sediments may be expelled in fluids as the downgoing slab is metamorphosed and accumulate in the overlying mantle wedge (Barreiro, 1984). The igneous rocks have homogeneous and generally low $^{87}\text{Sr}/^{86}\text{Sr}$ ratios, and $^{143}\text{Nd}/^{144}\text{Nd}$ above that of bulk earth, similar to the values of present-day intra-oceanic island arcs (Figure 5) and in agreement with the Pb isotope data. These results suggest a relatively low degree of evolved crustal contamination, but are consistent with involvement of subducted sediment. Differences between rocks from La Verde and Ingurán, El Malacate, and La Esmeralda could result from assimilation of different rocks (Arteaga Complex or sedimentary rocks) or different extents of contamination.

West of the study area, the late Cretaceous granitoid complexes from Puerto Vallarta (~80–100 Ma), Manzanillo, and Jilotlán (~65 Ma) (Schaaf *et al.*, 1995; Ducea *et al.*, 2004; Morán-Zenteno *et al.*, 2007) (Figure 3) intruded Late Triassic to Early Cretaceous volcano-sedimentary arc units of the Zihuatanejo Sequence, located on the southern part of the Guerrero terrane (Freydier *et al.*, 1997). The Puerto Vallarta intrusives have lower ϵ_{Nd} values and higher $^{87}\text{Sr}/^{86}\text{Sr}$ ratios compared to the Manzanillo and Jilotlán complexes (Figure 8). These two different trends are surprising, considering that the batholiths intruded rocks

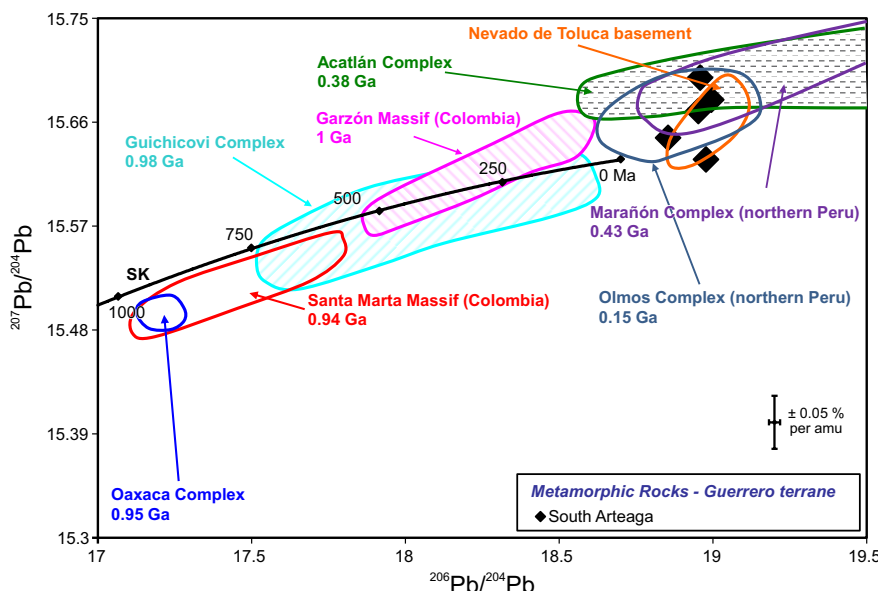


Figure 7. Present-day whole rock Pb isotope compositions of metamorphic rocks from the Guerrero terrane compared with reference data for the Mixteca (Martiny *et al.*, 1997) and the Oaxaca (Martiny *et al.*, 2000) terranes; Toluca metamorphic rocks (Martínez-Serrano *et al.*, 2004); the Santa Marta and Garzón Massifs (Colombia) and the Guichicovi Complex (Ruiz *et al.*, 1999); and the Olmos and Marañón Complexes (northern Peru) (Macfarlane and Petersen, 1990). SK represents the Stacey and Kramers (1975) average crustal Pb isotopic evolution curve. Also shown are the isotopic ages of the basement exposures.

of the same Zihuatanejo-Huetamo subterrane. Freydier *et al.* (1997) argued for the emplacement of the Puerto Vallarta batholith on an oceanic crust thickened by continent-derived sediments or a continental lithosphere as an explanation for the more evolved isotopic signatures. On the contrary, the positive ϵ_{Nd} values and lower $^{87}\text{Sr}/^{86}\text{Sr}$ ratios in the SE intrusions (Manzanillo and Jilotlán; Figure 8) suggest younger basement rocks and less crustal contamination (Schaaf *et al.*, 1990). The isotopic values of the Manzanillo and Jilotlán complexes overlap partly with the field defined by the arc-related rocks of the Guerrero

terrane and plot very close to the igneous samples from Inguarán, El Malacate, and La Esmeralda (Figure 8; Table 3). This similarity may indicate that they had a common source or that they were contaminated by assimilation of materials from the accreted arc volcanic and volcaniclastic rocks of the Guerrero terrane. However, Solís-Pichardo *et al.* (2008) argued for a mantle origin associated with Cordilleran subduction processes for the SE continental arc intrusives to account for their relatively primitive Sr and Nd isotopic ratios (Figure 8). Schaaf *et al.* (1991) suggested a multicomponent and multistage magma evolu-

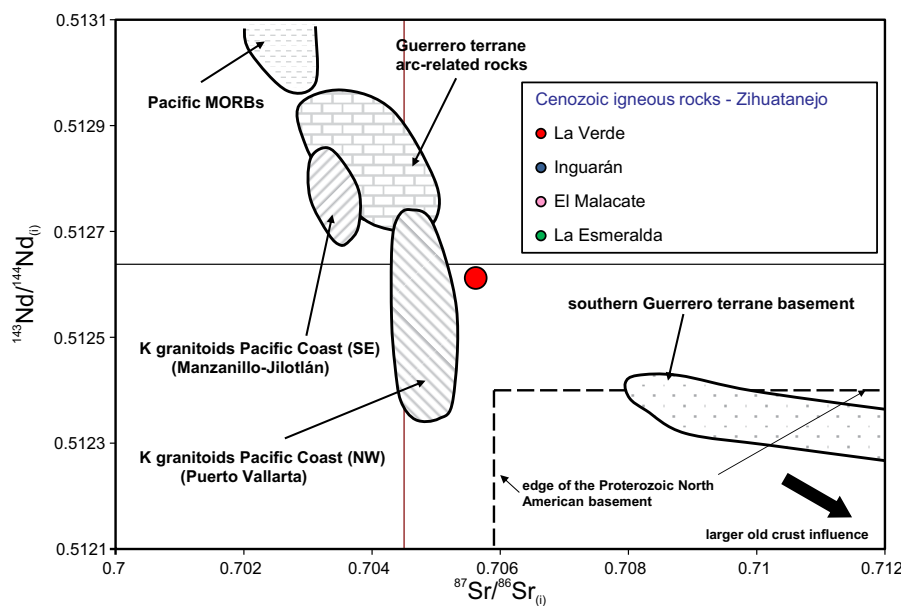


Figure 8. Sr-Nd isotopic correlation diagram for Cenozoic igneous rocks collected from the Zihuatanejo terrane. The compositional fields for Cretaceous granitoids along the Pacific coast (Schaaf *et al.*, 1990; Schaaf *et al.*, 1991), Guerrero terrane arc-related rocks (Centeno-García *et al.*, 1993a; Mendoza and Suárez, 2000), basement from the southern part of the Guerrero terrane (Centeno-García *et al.*, 1993a; Elías-Herrera *et al.*, 2003), and Pacific MORBs are also shown.

tion as an explanation for the heterogeneous $\varepsilon_{\text{Nd(i)}}$ (between -7 and +3) and less uniform Nd model ages (T_{DM} between 500 and 1400 Ma) of the Puerto Vallarta intrusives. On the basis of the more homogeneous isotopic signature and more uniform Nd model ages (T_{DM} between 250 and 500 Ma), the same authors argued for a single-stage magma generation for the SE granitoids.

The overall nonradiogenic $^{87}\text{Sr}/^{86}\text{Sr}$ ratios and $^{143}\text{Nd}/^{144}\text{Nd}$ above that of bulk earth of Jurassic-Cretaceous arc-related rocks from Guerrero terrane (Mendoza and Suástequi, 2000; Centeno-García *et al.*, 1993a; Figure 8) are similar to the values of present-day intra-oceanic island arcs (Figure 5). They have lower initial $^{87}\text{Sr}/^{86}\text{Sr}$ and higher initial $^{143}\text{Nd}/^{144}\text{Nd}$ than basement rocks (*e.g.*, the Arteaga Complex; Figure 8), suggesting that the basement rocks did not influence the magmatism and were not involved in the production of the Jurassic-Cretaceous arc assemblage (Centeno-García *et al.*, 1993a).

CONCLUSIONS

We conclude that Pb isotope compositions of the Mexican basement rocks more closely resemble those of the northern part of South America (Colombia and northern Peru) than exposures from North America: the Oaxaca Complex (Mexico) is similar to the Santa Marta Massif (Colombia), the Guichicovi Complex (Mexico) is similar to the Garzón Massif (Colombia), and the Acatlán, Arteaga, and Tejupilco Complexes (Mexico) are similar to the Olmos and Marañón Complexes (northern Peru). Common occurrences of high $^{206}\text{Pb}/^{204}\text{Pb}$ are present on the western side of Mexico (Nevado de Toluca xenoliths, and exposures of the Arteaga Complex and Acatlán Complex) and northern Peru (with exposures of the Olmos and Marañón complexes), whereas areas of low $^{206}\text{Pb}/^{204}\text{Pb}$ are located on the southeastern part of Mexico (with exposures of the Oaxaca and Guichicovi complexes) and Colombia (Santa Marta and Garzón massifs). The radiogenic Pb in rocks from the Mixteca terrane, Guerrero terrane, and the north Peruvian complexes, reflecting a history of elevated U/Pb relative to bulk earth models, reveal a different history from that of the ancient Oaxaca terrane, Guichicovi Complex, and the Colombian massifs, which reflect variable depletion of U relative to Pb.

The sedimentary rocks from the Zihuatanejo terrane, represented by two isotopically-distinct sequences, seem to have originated from different sources. Samples from the Huetamo area, the less radiogenic ones, appear to be the result of mixing between oceanic basalts and

a small input of radiogenic material from the basement rocks represented by the Arteaga Complex. Rocks from the Coastal belt area of the Zihuatanejo terrane have higher isotopic ratios, which can be explained by input of material from a more radiogenic member or input of a higher percentage of radiogenic component compared to rocks from the Huetamo region. Sedimentary samples from the Teloloapan terrane have similar Pb, Sr, and Nd isotopic compositions to samples from the Coastal belt area of the Zihuatanejo terrane, suggesting similar sources.

Overall, it is apparent that there was involvement of crustal material at some stage in the evolution of the subduction-related Cenozoic igneous rocks. This could be by assimilation during the rise of the magma, or by incorporation of subducted sediments, or both. Assimilation of crustal material during magma ascent is a possibility in the Guerrero terrane, where the igneous rocks were emplaced through the Mesozoic metamorphic basement. The slightly higher Pb and Sr isotope ratios of the igneous rocks from La Verde may be the result of contamination with older crustal components to a larger extent than the igneous rocks from Ingurán, La Esmeralda, and El Malacate, or a greater extent of assimilation. Current data indicate that igneous rocks from La Verde may have assimilated a more evolved crustal component than any other magmatic rock from southern Mexico.

ACKNOWLEDGMENTS

We would like to thank Víctor de la Garza for organizing the field work that allowed collection of the samples. The project was also facilitated by Roberto Tellez and Arturo Broca who took care of the logistical arrangements, and by Sergio Rodríguez who provided local knowledge and geological expertise. A. Sachi-Kocher and T. Trejos assisted with laboratory work carried out at the National High Magnetic Field Laboratory in Tallahassee and at the Trace Evidence Analysis Facility in Miami, respectively. Florida International University's Graduate School provided A. Potra with the 2008 Doctoral Evidence Acquisition Fellowship and the 2010 Dissertation Year Fellowship, which largely made writing of this manuscript possible. We thank Elena Centeno-García (Instituto de Geología, Universidad Nacional Autónoma de México, UNAM), Alexander Iriondo (Centro de Geociencias, UNAM), Jonathan Patchett (The University of Arizona), and Peter Schaaf (Instituto de Geofísica, UNAM) for improving the paper through their insightful comments and critical reviews.

APPENDIX I Location and description of analyzed samples

Sample	Latitude (N)	Longitude (W)	Area	Material
Metamorphic rocks				
Zihuatanejo terrane	96MR101	18°19.361'	102°17.111'	South of Arteaga
	96MR102	18°19.361'	102°17.111'	South of Arteaga
	96MR103	18°19.361'	102°17.111'	South of Arteaga
	96MR105	18°18.879'	102°17.142'	South of Arteaga
	96MR107	18°18.406'	102°16.995'	South of Arteaga
Sedimentary rocks				
Zihuatanejo terrane – Coastal belt	96MR055	19°40.000'	104°04.000'	Northwest of Colima
	96MR057	19°40.000'	104°43.000'	Purificación area
	96MR067	19°03.570'	103°39.124'	South of Colima
	96MR068	19°03.570'	103°39.124'	South of Colima
	96MR069	19°03.570'	103°39.124'	South of Colima

continues

APPENDIX I (cont.)
Location and description of analyzed samples

	Sample	Latitude (N)	Longitude (W)	Area	Material
Sedimentary rocks (cont.)					
<i>Zihuatanajo terrane – Huetamo region</i>	96MR114	18°28.594'	100°43.091'	Between Altamirano and Huetamo	Shale
	96MR116	18°34.133'	100°50.085'	Between Altamirano and Huetamo	Siltstone
	96MR117	18°34.133'	100°50.085'	Between Altamirano and Huetamo	Siltstone
	96MR118	18°35.221'	100°56.717'	Between Altamirano and Huetamo	Red siltstone
	96MR119	18°35.221'	100°56.717'	Between Altamirano and Huetamo	Coarse-grained, red sandstone
	96MR121	18°32.412'	100°58.402'	Between Altamirano and Huetamo	Coarse-grained, red sandstone
	96MR127	18°40.511'	100°51.471'	Near Huetamo	Mudstone
	96MR128	18°40.332'	100°51.481'	Near Huetamo	Siltstone
<i>Teloloapan terrane</i>	96MR129	18°23.174'	100°14.722'	East of Arcelia	(meta)-Siltstone
	96MR131	18°23.754'	100°05.098'	South of Teloloapan	(meta)-Sandstone
	96MR133	18°22.547'	099°40.596'	Southeast of Teloloapan	(meta)-Siltstone
Igneous rocks					
<i>Zihuatanajo terrane</i>	96MR071	19°05.098'	102°02.880'	La Verde - mine area; West Hill	Potassically altered granodiorite
	96MR076	19°05.190'	102°02.748'	La Verde - mine area; East Hill	Altered and silicified diorite
	96MR078	19°04.904'	102°03.203'	La Verde - near the mine	Much fresher granodiorite
	96MR079	19°05.223'	102°02.044'	La Verde - mine area; East Hill	Altered, silicified granodiorite
	96MR083	19°05.038'	102°01.800'	La Verde - mine area	Fresh-looking granodiorite
	96MR088	19°09.460'	101°58.322'	La Verde - big quarry	Fresh granite
	96MR095	18°53.566'	101°38.600'	Inguarán	Massive granodiorite
	96MR096	18°54.003'	101°34.282'	El Malacate mine; altitude ~ 1300 m	Fresh granodiorite
	96MR099	18°53.502'	101°37.013'	La Esmeralda	Slightly altered granodiorite

APPENDIX II
Detailed analyses of USGS reference materials

Element	Avg. BIR-1	Avg. dev. (%)	Recommended	Bias	Avg. DNC-1	Avg. dev. (%)	Recommended	Bias
U	0.039	2.795	N/A**	-	0.081	2.020	N/A	-
Th	0.021	8.777	N/A	-	0.199	1.018	N/A	-
Pb	3.467	0.280	N/A	-	6.332	0.616	N/A	-
Rb	0.974	4.725	N/A	-	4.210	0.114	N/A	-
Sr	102.388	1.171	110±2	-6.9	138.479	0.188	144±1.8	-3.8
Sm	1.033	0.133	N/A	-	1.377	0.147	N/A	-
Nd	2.518	0.965	2.5±0.7	0.7	5.109	0.675	5.2±0.56	-1.8
Element	Avg. BHVO-2	Avg. dev. (%)	Recommended	Bias	Avg. AGV-2	Avg. dev. (%)	Recommended	Bias
U	0.433	1.070	N/A	-	1.883	1.284	1.88±0.16	0.2
Th	1.145	0.810	N/A	-	5.991	0.686	6.1±0.6	-1.8
Pb	2.129	0.033	N/A	-	12.947	0.653	13±1	-0.4
Rb	9.611	0.968	9.8±1	-1.9	67.260	0.707	68.6±2.3	-2
Sr	397.831	0.031	389±23	2.3	678.608	0.130	658±17	3.1
Sm	6.246	0.211	N/A	-	5.807	0.251	N/A	-
Nd	24.706	0.546	25±1.8	-1.2	31.321	0.851	30±2	4.4
Element	Avg. W-2	Avg. dev. (%)	Recommended	Bias	Avg. QLO-1	Avg. dev. (%)	Recommended	Bias
U	0.505	0.170	N/A	-	1.872	0.520	1.9±0.12	-1.5
Th	2.240	0.329	2.4±0.1	-6.6	4.691	0.410	4.5±0.5	4.1
Pb	8.289	0.011	N/A	-	19.871	0.351	20±0.8	-0.6
Rb	19.973	0.381	21±1.1	-4.9	71.570	0.157	74±3	-3.3
Sr	187.811	0.112	190±3	-1.2	345.910	1.554	340±12	1.7
Sm	3.343	0.808	3.3±0.13	1.3	4.850	0.449	4.9±0.2	-1
Nd	13.272	0.270	13±1	2.1	23.954	0.181	N/A	-

* Source of data: http://crustal.usgs.gov/geochemical_reference_standards/powdered_RM.html.

** N/A = no recommended data are available, only information values or no values.

REFERENCES

Alvarez, J., Cordani, U.G., 1980, Precambrian basement within the septentrional Andes: age and geological evolution, in XXVI International Geologic Congress: Paris, Abstracts, 1, 18-19.

Barreiro, B.A., 1984, Lead isotopes and Andean magmagenesis, in Harmon, R.S., Barreiro, B.A. (eds.), Andean Magmatism, chemical and isotopic constraints: Cheshire, Shiva, 21-30.

Barton, M.D., Staude, J.M., Zurcher, L., Megaw, P.K.M., 1995, Porphyry copper and other intrusion-related mineralization in Mexico, in Pierce, F.W., Bolm, J.G. (eds.), Porphyry copper deposits of the American Cordillera: Arizona Geological Society Digest, 20, 487-524.

Ben-Avraham, Z., 1989, Introduction: The evolution of the Pacific Ocean margins, in Ben-Avraham, Z. (ed.), The Evolution of the Pacific Ocean Margins: Oxford Monographs on Geology and Geophysics 8, Oxford University Press, New York, 3-4.

Burckhardt, C., Scalia, S., 1906, Geologie des environs de Zacatecas: Guide des excursions, in Décimo Congreso Geológico Internacional: México, Distrito Federal, 16, 1-26.

Cabral-Cano, E., Draper, G., Lang, H.R., Harrison, C.G.A., 2000, Constraining the Late Mesozoic and Early Tertiary tectonic evolution of southern Mexico: structure and deformation history of the Tierra Caliente region: The Journal of Geology, 108, 427-446.

Campa, M.F., Coney, P.J., 1983, Tectono-stratigraphic terranes and mineral resource distributions in Mexico: Canadian Journal of Earth Sciences, 20, 1040-1051.

Campa-Uranga, M.F., Ramírez-Espinosa, J., 1979, La Evolución Geológica y la Metalogénesis del Noroccidente de Guerrero: Universidad Autónoma de Guerrero, Serie Técnico-Científica, 1, 84 pp.

Campa, M.F., Ramírez, J., Bloome, C., 1982, La secuencia volcánico-sedimentaria metamorfizada del Triásico (Ladiniano-Cárlico) de la región de Tumbiscatío, Michoacán, in VI Convención Geológica Nacional: Sociedad Geológica Mexicana, Resúmenes, 48.

Centeno-García, E., 2005, Review of Upper Paleozoic and Lower Mesozoic stratigraphy and depositional environments of central and west Mexico: Constraints on terrane analysis and paleogeography, in Anderson, T.H., Nourse, J.A., McKee, J.W., Steiner, M.B. (eds.), The Mojave-Sonora Megashare Hypothesis: Development, Assessment, and Alternatives: Geological Society of America Special Paper, 393, 233-258.

Centeno-García, E., Silva-Romo, G., 1997, Petrogenesis and tectonic evolution of central Mexico during Triassic-Jurassic time: Revista Mexicana de Ciencias Geológicas, 14(2), 244-260.

Centeno-García, E., Ruiz, J., Coney, P.J., Patchett, J.P., Ortega-Gutiérrez, F., 1993a, Guerrero Terrane of Mexico: Its role in the Southern Cordillera from new geochemical data: Geology, 21, 419-422.

Centeno-García, E., García, J.L., Guerrero-Suástequi, M., Ramírez-Espinosa, J., Salinas-Prieto, J.C., Talavera-Mendoza, O., 1993b, Geology of the southern part of the Guerrero Terrane, Ciudad Altamirano-Teloloapan area, in Ortega-Gutiérrez, F., Coney, P., Centeno-García, E., Gómez-Caballero, A. (eds.), Terrane Geology of Southern Mexico: First Circum-Pacific and Circum-Atlantic Terrane Conference, Guidebook of Field Trip B, Guanajuato, Mexico: Mexico D.F., Universidad Nacional Autónoma de México, Instituto de Geología, 22-33.

Centeno-García, E., Corona-Chávez, P., Talavera-Mendoza, O., Iriondo, A., 2003, Geologic and tectonic evolution of the western Guerrero terrane – a transect from Puerto Vallarta to Zihuatanejo, Mexico, in Alcayde, M., Gómez-Caballero, A. (eds.), Geologic transects across Cordilleran Mexico: Guidebook for the field trips of the 99th Geological Society of America Cordilleran Section Annual Meeting: Puerto Vallarta, Jalisco, Mexico, April 4-7, 2003, Universidad Nacional Autónoma de México, Instituto de Geología, Special Paper, 1, 201-228.

Centeno-García, E., Guerrero-Suástequi, M., Talavera-Mendoza, O., 2008, The Guerrero composite terrane of western Mexico: Collision and subsequent rifting in a supra-subduction zone, in Draut, A.E., Clift, P.D., Scholl, D.W. (eds.), Formation and applications of the sedimentary record in arc collision zones: Geological Society of America Special Paper, 436, 279-308.

Centeno-García, E., Busby, C., Busby, M., Gehrels, G., 2011, Evolution of the Guerrero composite terrane along the Mexican margin, from extensional fringing arc to contractional continental arc: Geological Society of America Bulletin, 123, 1776-1797.

Coney, P.J., 1989, The North American Cordillera, in The Evolution of the Pacific Ocean Margins: Oxford Monographs on Geology and Geophysics 8, Oxford University Press, New York, 43-52.

Coney, P.J., Jones, D.L., Monger, J.W.H., 1980, Cordilleran suspect terranes: Nature, 188, 329-333.

Coochey, D.V., Eckman, P., 1978, Geology of the La Verde copper deposits, Michoacán, Mexico: Arizona Geological Society Digest, 11, 129-137.

DePaolo, D.J., 1981, Neodymium isotopes in the Colorado Front Range and crust-mantle evolution in the Proterozoic: Nature, 291, 193-196.

Dickinson, W.R., Lawton, T., 2001, Carbonaceous to Cretaceous assembly and fragmentation of Mexico: Geological Society of America Bulletin, 113, 1142-1160.

Ducea, M.N., Gehrels, G.E., Shoemaker, S., Ruiz, J., Valencia, V.A., 2004, Geologic evolution of the Xolapa Complex, southern Mexico: Evidence from U-Pb zircon geochronology: Geological Society of America Bulletin, 116, 1016-1025.

Elías-Herrera, M., Sánchez-Zavala, J.L., 1990 (1992), Tectonic implications of a mylonitic granite in the lower structural levels of the Tierra Caliente complex (Guerrero terrane), southern Mexico: Universidad Nacional Autónoma de México, Instituto de Geología, Revista Mexicana de Ciencias Geológicas, 9(2), 113-125.

Elías-Herrera, M., Ortega-Gutiérrez, F., Cameron, K.L., 1996, Pre-Mesozoic continental crust beneath the southern Guerrero terrane: xenolith evidence: GEOS, Unión Geofísica Mexicana, Resúmenes y Programas de la Reunión Anual, 16, 234.

Elías-Herrera, M., Sánchez-Zavala, J.L., Macías-Romo, C., 2000, Geologic and geochronologic data from the Guerrero Terrane in the Tejupilco area, southern Mexico: new constraints on its tectonic interpretation: Journal of South American Earth Sciences, 13, 355-375.

Elías-Herrera, M., Ortega-Gutiérrez, F., Sánchez-Zavala, J.L., Macías-Romo, C., 2003, The real Guerrero Terrane, southern Mexico: new insights from recent studies, in Geological Society of America, Cordilleran Section, 99th annual meeting, Puerto Vallarta, Jal., Mexico: EUA, Geological Society of America, Abstracts with Programs 35, 66.

Freydier, C., Talavera-Mendoza, O., Tardy, M., Lapierre, H., Coulon, C., Ortiz, E., Yta, M., Martínez, J., 1993, Birth, growth and accretion of Mesozoic intra-oceanic island arc (Guerrero Terrane), in Proceedings of the First Circum-Pacific and Circum-Atlantic Terrane Conference, Guanajuato, Mexico: México, D.F., Universidad Nacional Autónoma de México, Instituto de Geología, 50-51.

Freydier, C., Lapierre, H., Briqueu, L., Tardy, M., Coulon, C., Martínez-Reyes, J., 1997, Volcaniclastic sequences with continental affinities within the Late Jurassic-Early Cretaceous Guerrero intra-oceanic arc terrane (western Mexico): Journal of Geology, 105, 483-502.

Grajales, M., López, M., 1984, Estudio petrogenético de las rocas ígneas y metamórficas en el Prospecto Tomatlán-Guerrero-Jalisco: Instituto Mexicano del Petróleo, Subdirección de Tecnología y Exploración, Proyecto C-1160 (unpublished report).

Guerrero, M., Ramírez, J., Talavera, O., 1990, Estudio estratigráfico del arco volcánico Cretácico Inferior de Teloloapan, Guerrero, in X Convención Geológica Nacional: Sociedad Geológica Mexicana, Resúmenes, 67.

Guerrero-Suástequi, M., 1997, Depositional history and sedimentary petrology of the Huetamo sequence, Southwestern Mexico: University of Texas at El Paso, M. Sc. Thesis, 240 pp.

Guerrero-Suástequi, M., 2004, Depositional and tectonic history of the Guerrero Terrane, Sierra Madre del Sur, with emphasis on sedimentary successions of the Teloloapan area, southwestern Mexico: St. John's, Memorial University of Newfoundland, Ph.D. Thesis, 332 pp.

Guerrero-Suástequi, M., Ramírez-Espinosa, J., Talavera-Mendoza, O., Campa-Uranga, M.F., 1991, El desarrollo carbonatado del Cretácico Inferior asociado al arco de Teloloapan, Noroccidente del Estado de Guerrero, in Convención sobre la Evolución Geológica Mexicana, 1er Congreso Mexicano de Mineralogía: Pachuca, México, Memorias, 67-70.

Hart, S.R., Brooks, C., 1977, The geochemistry and evolution of early Precambrian mantle: Contributions to Mineralogy and Petrology, 61, 109-128.

Hemming, S.R., McLennan, S.M., 2001, Pb isotope compositions of modern deep sea turbidites: Earth and Planetary Science Letters, 184, 489-503.

Howell, D.G., Jones, D.L., 1989, Terrane analysis: a Circum-Pacific overview, in Ben-Avraham, Z. (ed.), *The Evolution of the Pacific Ocean Margins: Oxford Monographs on Geology and Geophysics 8*, Oxford University Press, New York, 36-40.

Howell, D.G., Schermer, E.R., Jones, D.L., Ben-Avraham, Z., Scheibner, E., 1983, Tectonostratigraphic Terrane Map of the Circum-Pacific Region: Menlo Park, California, United States Geological Survey Open-File Report 83-716.

King, P.B., 1959, *The evolution of North America*: New Jersey, Princeton University Press, 189 pp.

Lang, H.R., Barros, T., Cabral-Cano, E., Draper, G., Jansma, P., Johnson, C., 1996, Terrane deletion in northern Guerrero: *Geofísica Internacional*, 35, 349-359.

Lapierre, H., Ortiz, L.E., Abouchami, W., Monod, O., Coulon, C., Zimmermann, J.L., 1992, A crustal section of an intra-oceanic island arc: the Late Jurassic – Early Cretaceous Guanajuato magmatic sequence, central Mexico: *Earth and Planetary Science Letters*, 108, 61-77.

Macfarlane, A.W., 1999, Isotopic studies of Northern Andean crustal evolution and ore metal sources: *Society of Economic Geologists Special Publication Series*, 7, 195-217.

Macfarlane, A.W., Petersen, U., 1990, Pb isotopes of the Hualgayoc area, northern Peru: Implications for metal provenance and genesis of a Cordilleran polymetallic mining district: *Economic Geology*, 85, 1303-1327.

Manhes, G., Minster, J.F., Allegre, C.J., 1978, Comparative uranium-thorium-lead and rubidium-strontium study of the Saint Severin amphotericite: consequences for early solar system chronology: *Earth and Planetary Science Letters*, 39, 14-24.

Martínez-Serrano, R.G., Schaaf, P., Solís-Pichardo, G., Hernández-Bernal, M., Hernández-Treviño, T., Morales-Contreras, J., Macías, J.L., 2004, Sr, Nd and Pb isotope and geochemical data from the Quaternary Nevado de Toluca Volcano, a source of recent adakitic magmatism, and the Tenango volcanic field, Mexico: *Journal of Volcanology and Geothermal Research*, 138, 77-110.

Martini, M., Ferrari, L., López-Martínez, M., Cerca-Martínez, M., Valencia, V., Serrano-Durán, L., 2009, Cretaceous-Eocene magmatism and Laramide deformation in Southwestern Mexico: No role for terrane accretion, in Kay, S.M., Ramos, V.A., Dickinson, W.R. (eds.), *Backbone of the Americas, shallow subduction, plateau uplift, and ridge and terrane collision: Geological Society of America Memoir*, 204, 151-182.

Martini, M., Ferrari, L., López-Martínez, M., Valencia, V., 2010, Stratigraphic redefinition of the Zihuatanejo area, southwestern Mexico: *Revista Mexicana de Ciencias Geológicas*, 27(3), 412-430.

Martini, M., Mori, L., Solari, L., Centeno-García, E., 2011, Sandstone Provenance of the Arperos Basin (Sierra de Guanajuato, Central Mexico): Late Jurassic-Early Cretaceous Back-Arc Spreading as the Foundation of the Guerrero Terrane: *The Journal of Geology*, 119, 597-617.

Martini, M., Solari, L., Camprubi, A., 2012, Kinematics of the Guerrero terrane accretion in the Sierra de Guanajuato, central Mexico: new insights for the structural evolution of arc-continent collisional zones: *International Geology Review*, 55, 574-589.

Martiny, B., Martínez-Serrano, R., Ayuso, R.A., Macías-Romo, C., Morán-Zenteno, D.J., Alba-Aldave, L., 1997, Pb isotope geochemistry of Tertiary igneous rocks and continental crustal complexes, southern Mexico: *EOS Transactions, American Geophysical Union* 78, 844.

Martiny, B., Martínez-Serrano, R.G., Morán-Zenteno, D.J., Macías-Romo, C., Ayuso, R.A., 2000, Stratigraphy, geochemistry and tectonic significance of the Oligocene magmatic rocks of western Oaxaca, southern Mexico: *Tectonophysics*, 318, 71-98.

Mauger, R.L., McDowell, F.W., Blount, J.G., 1983, Grenville-age Precambrian rocks of Los Filtros area, near Aldama, Chihuahua, Mexico, in Clark, K.F., Goodell, P.C. (eds.), *Geology and mineral resources of north-central Chihuahua: El Paso Geological Society Guidebook*, 165-168.

McDowell, F.W., Keizer, R.P., 1977, Timing of mid-Tertiary volcanism in the Sierra Madre Occidental between Durango City and Mazatlán, Mexico: *Geological Society of America Bulletin*, 88, 1479-1487.

Mendoza, T.O., Suárez, G.M., 2000, Geochemistry and isotopic composition of the Guerrero Terrane (western Mexico): implications for the tectono-magmatic evolution of southwestern North America during the late Mesozoic: *Journal of South American Earth Sciences*, 13, 297-324.

Morán-Zenteno, D.J., Tolson, G., Martínez-Serrano, R.G., Martiny, B., Schaaf, P., Silva-Romo, G., Macías-Romo, C., Alba-Aldave, L., Hernández-Bernal, M.S., Solís-Pichardo, G., 1999, Tertiary arc-magmatism of the Sierra Madre del Sur, Mexico, and its transition to the volcanic activity of the Trans-Mexican Volcanic Belt: *Journal of South American Earth Sciences*, 12, 513-535.

Morán-Zenteno, D.J., Alba-Aldave, L.A., Sole, J., Iriondo, A., 2004, A major resurgent caldera in southern Mexico: the source of the late Eocene Tilzapota Ignimbrite: *Journal of Volcanology and Geothermal Research*, 136, 97-119.

Morán-Zenteno, D.J., Cerca, M., Keppie, J.D., 2007, The Cenozoic tectonic and magmatic evolution of southwestern Mexico: Advances and problems of interpretation, in Alaniz-Álvarez, S.A., Nieto-Samaniego, A.F. (eds.), *Geology of Mexico: Celebrating the centenary of the Geological Society of Mexico: Geological Society of America Special Paper*, 422, 71-91.

Mortensen, J.K., Hall, B.V., Bissig, T., Friedman, R.M., Danielson, T., Oliver, J., Rhys, D.A., Ross, K.V., Gabites, J.E., 2008, Age and paleotectonic setting of volcanogenic massive sulfide deposits in the Guerrero Terrane of central Mexico: Constraints from U-Pb age and Pb isotope studies: *Economic Geology*, 103, 117-140.

Nelson, B.K., Bentz, K.L., 1990, Isotopic and trace element evidence for the provenance of metagraywackes from the Franciscan Complex, CA: *EOS Transactions, American Geophysical Union* 71, 1689.

Ortega-Gutiérrez, F., 1981, Metamorphic belts of southern Mexico and their tectonic significance: *Geofísica Internacional*, 20, 177-202.

Ortega-Gutiérrez, F., Anderson, T.H., Silver, L.T., 1977, Lithologies and geochronology of the Precambrian craton of southern Mexico: *Geological Society of America, Abstracts with Programs* 9, 1121-1122.

Pantoya-Alor, J., 1959, Estudio Geológico de reconocimiento de la región de Huetamo, Estado de Michoacán: *Consejo de Recursos Naturales no Renovables – Boletín*, 50, 1-33.

Pantoya-Alor, J., Gómez-Caballero, J.A., 2003, Geologic features and biostratigraphy of the Cretaceous of southwestern Mexico (Guerrero Terrane), in Alcayde, M., Gómez-Caballero, A. (eds.), *Geologic transects across Cordilleran Mexico, Guidebook for the field trips of the 99th Geological Society of America Cordilleran Section Annual Meeting, Puerto Vallarta, Jalisco, Mexico, April 4-7, 2003*: Universidad Nacional Autónoma de México, Instituto de Geología, Special Paper 1, 229-260.

Patchett, P.J., Ruiz, J., 1987, Nd isotopic ages of crust formation and metamorphism in the Precambrian of eastern and southern Mexico: *Contributions to Mineralogy and Petrology*, 96, 523-528.

Potra, A., Macfarlane, A.W., 2014, Lead isotope studies of the Guerrero composite terrane, west-central Mexico: implications for ore genesis: *Mineralium Deposita*, 49, 101-117.

Ramírez-Espinoza, J., Campa, M.F., Talavera, O., Guerrero, M., 1991, Caracterización de los arcos insulares de la Sierra Madre del Sur y sus implicaciones tectónicas: *Convención sobre la Evolución Geológica de México, Primer Congreso Mexicano de Mineralogía, Memoria: Pachuca, Hgo., Mexico, Instituto de Geología, UNAM*, 163-166.

Restrepo-Pace, P., Ruiz, J., Gehrels, G.E., Cosca, M., 1997, Geochronology and Nd isotopic data of Grenville-age rocks in the Colombian Andes: new constraints for late Proterozoic-early Paleozoic paleocontinental reconstructions of the Americas: *Earth and Planetary Science Letters*, 150, 427-441.

Richard, P., Shimizu, N., Allegre, C.J., 1976, $^{143}\text{Nd}/^{146}\text{Nd}$, a natural tracer: an application to oceanic basalts: *Earth and Planetary Science Letters*, 31, 269-278.

Ruiz, J., Patchett, P.J., Ortega-Gutiérrez, F., 1988a, Proterozoic and Phanerozoic basement terranes of Mexico from Nd isotopic studies: *Geological Society of America Bulletin*, 100, 274-281.

Ruiz, J., Patchett, P.J., Arculus, R.J., 1988b, Nd - Sr isotope composition of lower crustal xenoliths: evidence for the origin of mid-Tertiary felsic volcanics in Mexico: *Contributions to Mineralogy and Petrology*, 99, 36-43.

Ruiz, J., Tosdal, R.M., Restrepo, P.A., Murillo-Mufietón, G., 1999, Pb isotope evidence for Colombia-southern Mexico connections in the Proterozoic, in Ramos, V.A., Keppie, J.D. (eds.), *Laurentia-Gondwana Connections before Pangea: Geological Society of America Special Paper*, 336, 183-197.

Schaaf, P., Kohler, H., Müller-Sohnius, D., Von Drach, V., 1990, Rb-Sr, Sm-Nd and K-Ar data on granitoids from the Pacific coast of Mexico between

21 degrees and 17 degrees N, in Seventh International Conference on Geochronology, Cosmochronology and Isotope Geology: Canberra, Australia, Geological Society of Australia, Abstracts Volume, 27, 89.

Schaaf, P., Kohler, H., Muller-Sohnius, D., Von Drach, V., Negendank, J.F.W., 1991, Sr-Nd and K-Ar data on age and genesis of West-Mexico Cordilleran batholiths, in Sixth Meeting of the European Unión of Geosciences: Strasbourg, Terra Abstracts, 3(1), 38.

Schaaf, P., Morán-Zenteno, D., Hernández-Bernal, M.S., Solís-Pichardo, G., Tolson, G., Kohler, H., 1995, Paleogene continental margin truncation in southwestern Mexico: Geochronological evidence: Tectonics, 14, 1339-1350.

Sedlock, R.L., Ortega-Gutiérrez, F., Speed, R.C., 1993, Tectonostratigraphic Terranes of Mexico, in Sedlock, R.L., Ortega-Gutiérrez, F., Speed, R.C. (eds.), Tectonostratigraphic Terranes and Tectonic Evolution of Mexico: Geological Society of America Special Paper, 278, 2-74.

Stacey, J.S., Kramers, J.D., 1975, Approximation of terrestrial lead isotope evolution by a two-stage model: Earth and Planetary Science Letters, 26, 207-221.

Sundblad, K., Cumming, G.L., Krstic, D., 1991, Lead isotope evidence for the formation of epithermal gold quartz veins in the Chortis Block, Nicaragua: Economic Geology, 86, 944-959.

Talavera-Mendoza, O., 2000, Melange in southern Mexico: Geochemistry and metamorphism of the Las Ollas Complex (Guerrero Terrane): Canadian Journal of Earth Sciences, 13, 337-354.

Talavera-Mendoza, O., Ramírez-Espinoza, J., Guerrero-Suástequi, M., 1993, Geochemical evolution of the Guerrero Terrane: example of a Late Mesozoic multi-arc system, in Ortega-Gutiérrez, F., Coney, P.J., Centeno-García, E., Morán-Zenteno, D.J., Gómez-Caballero, D.J. (eds.), Proceedings of the First Circum-Pacific and Circum-Atlantic Terrane Conference, Guanajuato, Mexico: México, D.F., Universidad Nacional Autónoma de México, Instituto de Geología, 150-152.

Talavera-Mendoza, O., Ramírez, J., Guerrero M., 1995, Petrology and geochemistry of the Teloloapan subterrane: a Lower Cretaceous evolved intra-oceanic island arc: Geofísica Internacional, 34, 3-22.

Talavera-Mendoza, O., Ruiz, J., Gehrels, G.E., Valencia, V.A., Centeno-García, E., 2007, Detrital zircon U/Pb geochronology of southern Guerrero and western Mixteca arc successions (southern Mexico): New insights for the tectonic evolution of the southwestern North America during the late Mesozoic: Geological Society of America Bulletin, 119, 1052-1065.

Tardy, M., Lapierre, H., Freydier, C., Coulon, C., Gill, J.B., Mercier de Lepinay, B., Beck, C., Martínez, R.J., Talavera, M.O., Ortiz, H.E., Stein, G., Bourdier, J.L., Yta, M., 1994, The Guerrero suspect terrane (western Mexico) and coeval arc terranes (the Greater Antilles and the Western Cordillera of Colombia): a late Mesozoic intra-oceanic arc accreted to cratonal America during the Cretaceous: Tectonophysics, 230, 49-73.

Todt, W., Cliff, R.A., Hanser, A., Hofmann, A.W., 1996, Evaluation of a ^{202}Pb - ^{205}Pb double spike for high-precision lead isotope analysis, in Basu, R., Hart, S.R. (eds.), Earth processes: reading the isotopic code: American Geophysical Unión Monograph, 95, 429-437.

Valencia-Moreno, M., Ruiz, J., Barton, M.D., Patchett, P.J., Zurcher, L., Hodgkinson, D.G., Roldan-Quintana, J., 2001, A chemical and isotopic study of the Laramide granitic belt of northwestern Mexico: Identification of the southern edge of the North American Precambrian basement: Geological Society of America Bulletin, 113, 1409-1422.

Verma, S.P., 2000, Geochemistry of the subducting Cocos Plate and the origin of subduction-unrelated mafic volcanism at the volcanic front of the central Mexican volcanic belt, in Delgado-Granados, H., Aguirre-Díaz, G.J., Stock, J.M. (eds.), Cenozoic tectonics and volcanism of Mexico: Geological Society of America Special Paper, 334, 195-222.

Vidal-Serratos, R., 1984, Tectónica de la región de Zihuatanejo, Guerrero, Sierra Madre del Sur, Mexico: Tesis Licenciatura, Escuela Superior de Ingeniería y Arquitectura, Instituto Politécnico Nacional, 155 pp.

White, W.M., Hofmann, A.W., Puchelt, H., 1987, Isotope geochemistry of Pacific mid-ocean ridge basalt: Journal of Geophysical Research, 92, 4881-4893.

Yañez, P., Ruiz, J., Patchett, P.J., Ortega-Gutiérrez, F., Gehrels, G.E., 1991, Isotopic studies of the Acatlán Complex, southern Mexico: Implications for Paleozoic North American tectonics: Geological Society of America Bulletin, 103, 817-828.

Zartman, R.E., Doe, B.R., 1981, Plumbotectonics - the model: Tectonophysics, 75, 135-162.

Manuscript received: August 28, 2013

Corrected manuscript received: January 27, 2014

Manuscript accepted: March 10, 2014